BMC Chemistry

RESEARCH

Open Access

Antimicrobial activity, synthesis, and docking study of some novel arylazo-1,3-thiazolopyrimidine and arylazo-1,3-thiazolopyridopyrimidine derivatives

Jihan Qurban[1], Sara A. Alqarni[2], Adel I. Alalawy[3], Nawaa Ali H. Alshammari[4], Gadeer R. S. Ashour[1], Maryam M. Alnoman[5], Hanadi A. Katuah[1] and Nashwa M. El-Metwaly[1,6*]

Abstract

In this study, a new series of aryl azo thiazolopyrimidine and thiazolopyridopyrimidine derivatives was synthesized using novel 6-aryl-4-(2,3,6,7-tetrahydro-*1H*,*5H*-pyrido[3,2,1-*ij*]quinolin-9-yl)-3,4-dihydropyrimidine-2(*1H*)-thione and 5-aryl-7-(2,3,6,7-tetrahydro-*1H*,*5H*-pyrido[3,2,1-ij]quinolin-9-yl)-2-thioxo-2,3-dihydropyrido[2,3-d]pyrimidin-4(*1H*)-one scaffolds as key intermediates. Structural elucidation of all intermediates and final products was performed via IR, UV, $^{1}H/^{13}C$-NMR, and mass spectrometry. Among the forty synthesized compounds, several exhibited significant in vitro antimicrobial activities, particularly derivatives **11a**, **11b**, **7a**, and **7b**, with potent inhibition against *S. aureus*, *E. coli*, and *C. albicans*. Molecular docking studies using the bacterial DNA gyrase B subunit (Protein Data Bank (PDB): 1aj6) revealed favorable binding interactions, especially for **11b**, which demonstrated the best docking score and strong π–H interactions. Furthermore, DFT-based molecular modeling confirmed the stability and high electronic reactivity of selected bioactive compounds, with low HOMO–LUMO energy gaps and favorable electrostatic potential profiles. Structure–activity relationship (SAR) analysis indicated that electronic effects, lipophilicity, and heteroaromatic substitution patterns critically influence antimicrobial potency. These findings support the potential of thiazolopyridopyrimidine derivatives as promising scaffolds for future antimicrobial drug development.

Keywords Chalcones, Pyrimidinethion derivatives, Antibacterial activity, Molecular docking

*Correspondence:
Nashwa M. El-Metwaly
n_elmetwaly00@yahoo.com; nmmohamed@uqu.edu.sa
[1] Department of Chemistry, College of Science, Umm Al-Qura University, 24230 Makkah, Saudi Arabia
[2] Department of Chemistry, College of Science, University of Jeddah, Jeddah, Saudi Arabia
[3] Department of Biochemistry, Faculty of Science, University of Tabuk, Tabuk, Saudi Arabia
[4] Department of Chemistry, College of Science, Northern Border University, 73222 Arar, Saudi Arabia
[5] Biology Department, Faculty of Science, Taibah University, Yanbu, Saudi Arabia
[6] Department of Chemistry, Faculty of Science, Mansoura University, El-Gomhoria Street 35516, Mansoura, Egypt

Introduction

Heterocyclic compounds form a significant class in organic chemistry due to their role as key components in many drugs, natural products, and chemicals used in daily life. These compounds are characterized by a cyclic structure that includes at least one heteroatom.

The most commonly used heteroatoms in heterocyclic compounds are oxygen, nitrogen, and sulfur [1]. Numerous pharmacological effects, including anticancer [2], antifungal [3–6], anti-inflammatory [7], anticonvulsant [8], and antibacterial [9–11] activity, are displayed by the heterocyclic compound. The pharmacological characteristics of pyrimidine derivatives, an important class of compounds, include antiviral [12], anticancer [13], antibacterial [14], and antihypertensive actions [15].

Aza-analogs of 1,4-dihydro pyridines, such as dihydropyrimidines (DHPMs), have garnered attention in recent times due to their comparable pharmacological profile to that of traditional dihydropyridine calcium channel modulators [16–18]. The dihydropyrimidines are widely known for their ability to inhibit calcium channels, but they are also being investigated for potential therapeutic benefits in the management of Acquired Immune Deficiency Syndrome (AIDS) [19]. This is because the natural marine alkaloids batzelladine A and B, which are the first low molecular weight natural products reported in the literature to inhibit the binding of Human immunodeficiency virus (HIV) gp-120 to CD4 cells, have been found to possess their specific structure [19]. This opens up a new avenue for the development of AIDS therapy.

Furthermore, fused thiazole is an important and widely utilized scaffold in the synthesis of new therapeutic agents and drugs. One class of anticancer medicines that is thought to be promising is fused thiazole scaffolds [20, 21]. The aryl group has a major impact on anticancer action, for example Dasatinib; nevertheless, improved activity may result from replacement at other places. Figure 1 lists a few of the marketed drugs with fused thiazole scaffolds and shows several anticancer drugs that are marketed and utilized in clinical trials that incorporate fused thiazole scaffolds.

Combining the two heterocyclic moieties, thiazole, and pyrimidine, is expected to enhance analgesic effects, as both are potent pharmacophores known for their activity against inflammation and pain. Thiazolopyrimidine derivatives have been synthesized previously [22, 23], and their pharmacological actions have been documented [24]. These derivatives are biosteric analogues of purines and may exhibit bioactivity with anti-inflammatory properties in vivo, similar to several common drugs while having minimal to no ulcerogenic effects [25, 26].

Furthermore, azo dyes have gained interest due to their various biological applications. They are thought to be incredibly resistant to xenobiotic substances and biodegradation processes. In 1932, the first drug based on sulphonamide was introduced to the market: protosil, a red azo dye. In pharmaceutics, the azo bond was used to protect drugs against undesirable side effects. An example of such a drug is Prontosil, a sulfonamide-based red azo dye, which was used for the treatment and prophylaxis of streptococcal infections in mice. Although Prontosil is inactive in vitro, it exhibits significant antibacterial effectiveness in vivo [27, 28].

Moreover, thieno[2,3-d]pyrimidines and pyrido[2,3-d] pyrimidines displayed antibacterial and antifungal activities [29–32]. Additionally, it was reported that julolidine-9-carbaldehyde, has remarkable biological activity [33].

The aim of the present study is to design, synthesize, and evaluate the antimicrobial potential of a series of novel arylazo-1,3-thiazolopyrimidine and arylazo-1,3-thiazolopyridopyrimidine derivatives. By integrating the biologically active thiazole, pyrimidine, and azo pharmacophores into a single molecular framework, this work seeks to discover new compounds with enhanced antibacterial and antifungal activities. Additionally, molecular docking studies were conducted to elucidate the interaction mechanisms of the most active compounds with bacterial protein targets, offering insights into their potential modes of action.

Results and discussion

Characterization of new synthesizes

The aim of this work is to focus on the utility of 6-aryl-4-(2,3,6,7-tetrahydro-1*H*,5*H*-pyrido[3,2,1-*ij*]quinolin-9-yl)−3,4-dihydropyrimidine-2(1*H*)-thione **(3)** and 5-aryl-7-(2,3,6,7-tetrahydro-1*H*,5*H*-pyrido[3,2,1-*ij*] quinolin-9-yl)−2-thioxo-2,3-dihydropyrido[2,3-*d*] pyrimidin-4(1*H*)-one **(4)** as precursors for the synthesis of aryl azo thiazolopyrimidine derivatives **6–13**. Compounds **3** and **4** were obtained by cyclocondensation of chalcones **2a-d** with 1,3-dinucleophiles (Scheme 1). Compounds **2a-d** were prepared by the reaction of julolidine-9-carbaldahyde with aryl acetyl derivatives **1a-d** by stirring at room temperature in the presence of alcoholic potassium hydroxide overnight. The reaction of chalcones **2a-d** with thiourea in boiling alcoholic potassium hydroxide afforded the corresponding pyrimidinethion derivatives **3a-d** (Schemes 1). The proposed mechanism (Scheme 2). Their IR spectra, in general, displayed absorption bands at ν 3310, and 3250 cm^{-1} for two NH groups, and around 1330 cm^{-1} characteristic for the C = S function group. The ^{1}H-NMR spectra revealed, in general, two doublet signals at δ 4.60 and 6.70 ppm for C_6-H, and C_5-H pyrimidine rings, respectively, in addition to a singlet signal at δ 7.00 ppm for two aromatic protons, a multiplet signals centred at δ 1.80 ppm for 2 CH_2 protons,

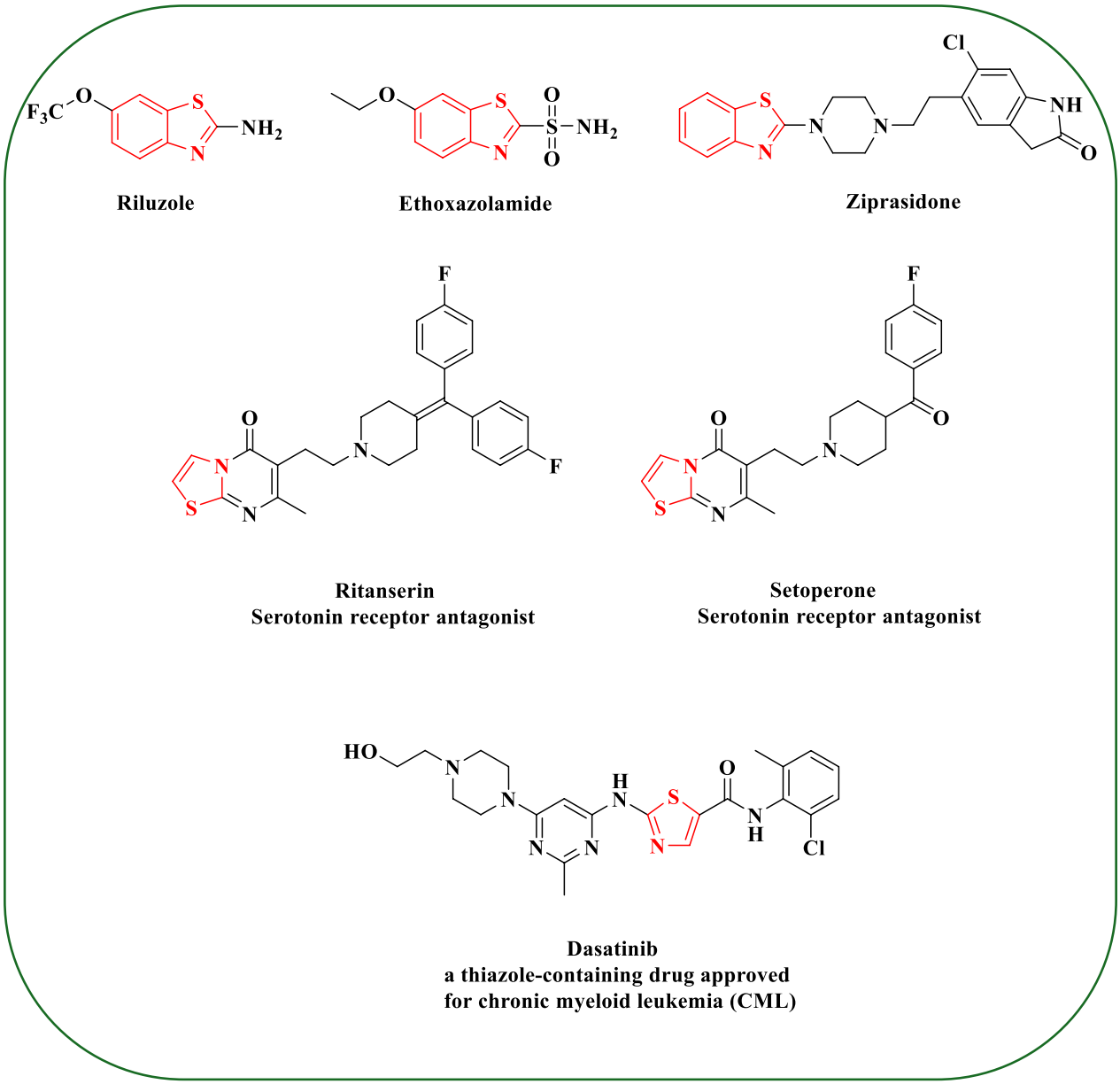

Fig. 1 Some marketed drugs of fused thiazole and thiazolopyrimidine derivatives

two triplet signals at δ 2.90 and 3.50 ppm of julolidine moiety, and finally two singlet signals at δ 9.68 and 12.50 ppm due to two NH groups.

On the other hand, chalones **2a-d** reacted with 6-amino-2-thioxo-2,3-dihydropyrimidine-4(1*H*)-one in boiling acetic acid to yield the corresponding pyridopyrimidines **4a-d** (Scheme 1). The proposed mechanism (Scheme 3). The IR spectra of compounds **4a-d**, in general, showed two NH and carbonyl groups at ν 3400, 3250, and 1670 cm^{-1}. The ^{1}H-NMR spectra, in general, displayed a singlet signal at δ 7.90 ppm attributable to pyridine-H and two aromatic H of julolidine moiety, and two NH signals at δ 12.50 and 13.80 ppm.

Additionally, fused thiazolopyrimidine derivatives **6–9** and thiazolopyridopyrimidine **10–13** were achieved via the reaction of **3a-d** and **4a-d** with hydrazonyl chloride **5a-d** [34–36] in absolute ethanol (schemes 4 and 5). The proposed mechanism for the synthesis of thiazolopyrimidine derivatives **6–9** (scheme 6). TLC analysis showed the presence of a sole reaction product. The structure of the above reaction products was established by their elemental and

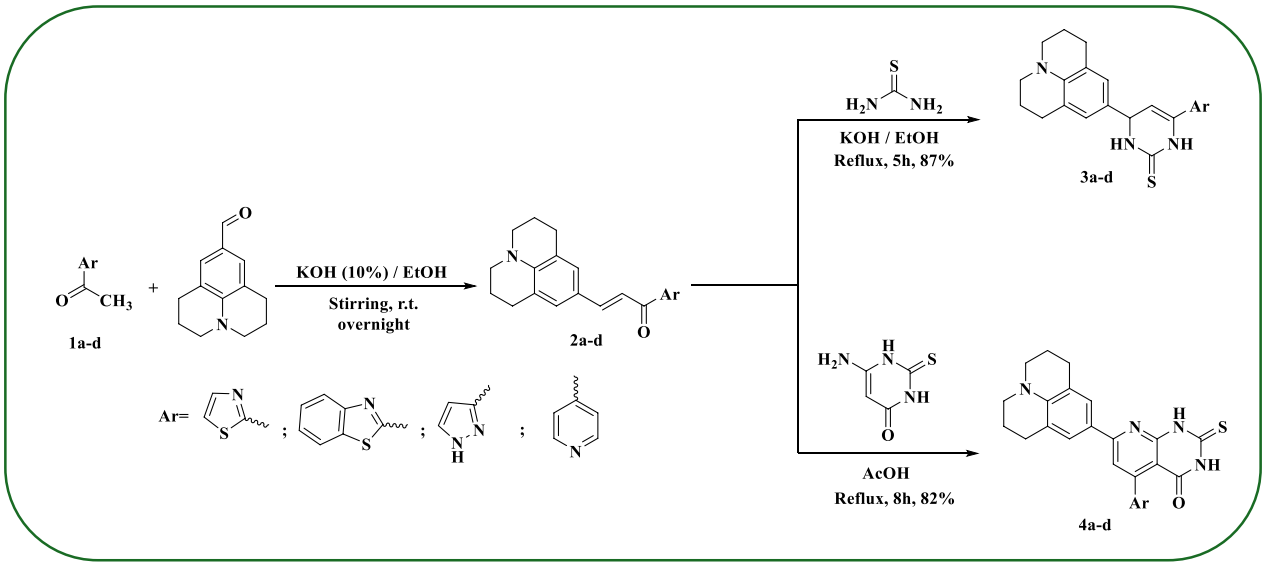

Scheme 1. Synthesis of chalcones derivatives **(2a-d)**, dihydropyrimidine-2(1H)-thione **(3)** and thioxo-2,3-dihydropyrido[2,3-d]pyrimidin-4(1H)-one **(4)**

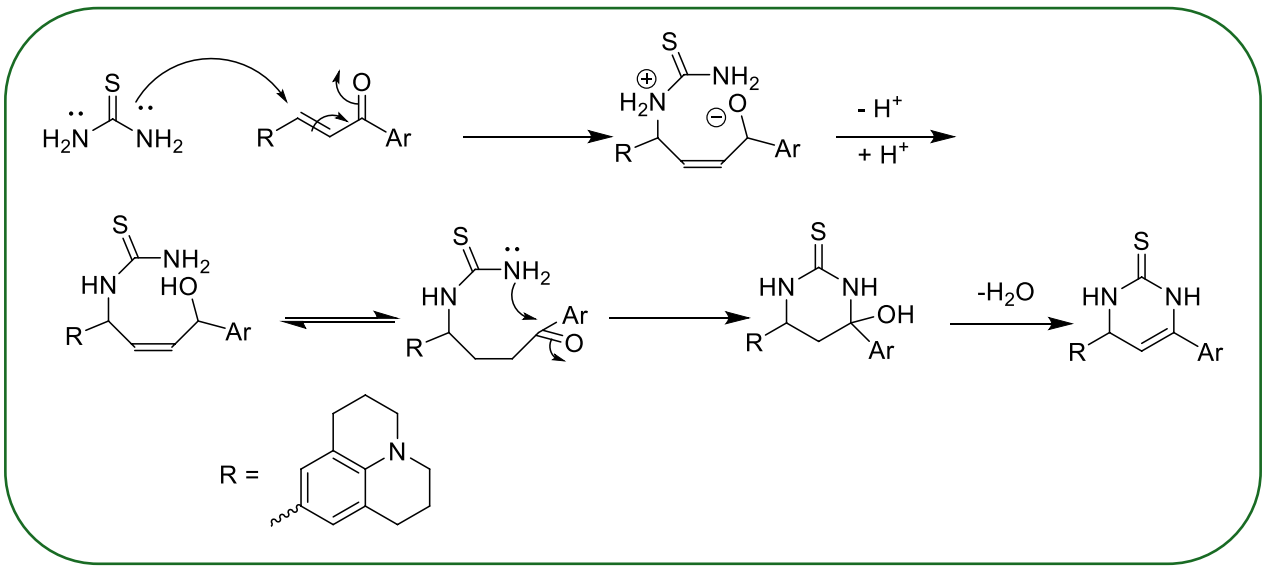

Scheme 2. The proposed mechanism for the synthesis of **3a-d**

spectral analyses. The IR spectrum of compounds **6–9** showed, in general, absorption bands at ν 1620, and 1550 cm^{-1} attributable to C = N and N = N functional groups, respectively. The ^{1}H-NMR of these compounds displayed, in general, a singlet signal at δ 2.30 ppm due to CH_3 protons, two doublets at δ 4.60 and 6.80 ppm of pyrimidine CH. In addition, the singlet signal at δ 7.02 ppm is due to aromatic protons of julolidine moiety. Moreover, two doublets at δ 7.20 and 7.40 ppm correspond to benzene protons (AB system).

On the other hand, the structure of compounds **10–13** was confirmed based on their elemental and spectral data. The IR spectra, in general, showed absorption bands at ν 1660, 1610, and 1555 cm^{-1} due to amidic carbonyl, C = N, and azo groups, respectively. While their ^{1}H-NMR spectra revealed, in general, a singlet signal at δ 2.30 ppm due to methyl proton, two doublets at δ 7.20, and 7.40 ppm due to benzene protons (AB system), a singlet signal at δ 8.00 of aromatic protons of julolidine moiety and finally, a singlet signal at

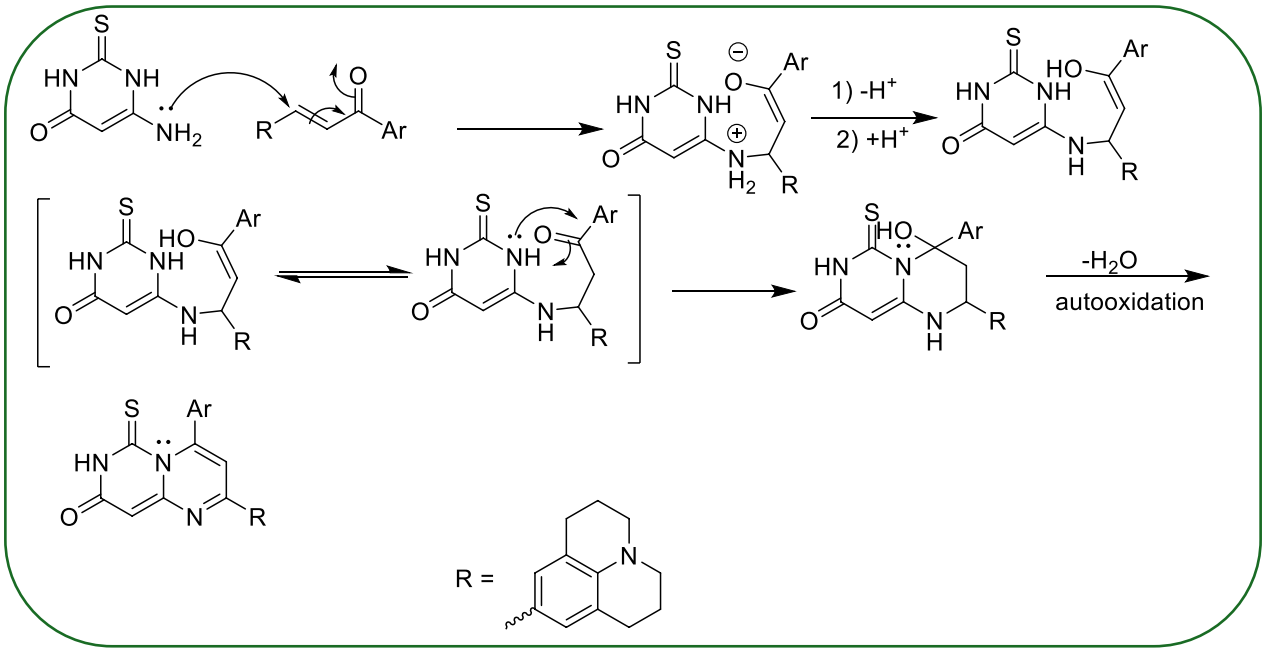

Scheme 3. The proposed mechanism for the synthesis of **4a-d**

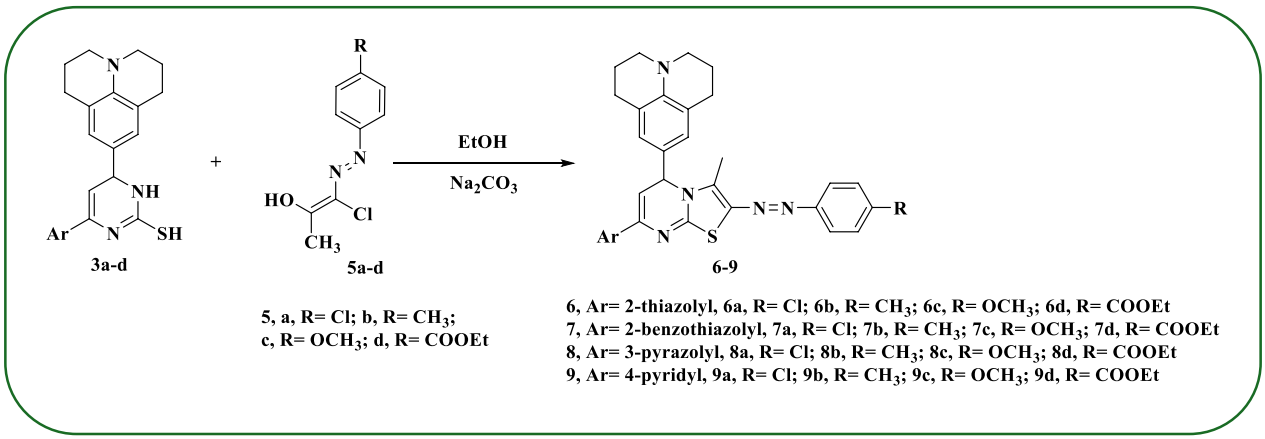

Scheme 4. Utility of hydrazonyl chloride **(5a-d)** in the synthesis of fused thiazolopyrimidine derivatives **6–9**

δ 8.50 due to pyridine CH. The ^{13}C-NMR spectra provide additional confirmation for the correct structure which showed a signal at δ 10.2, 22.1, and 28.1 ppm attributable to methyl and four CH_2 carbon atoms, a signal at δ 52.2 ppm due to CH_2-N-CH_2 carbon atoms. While the carbonyl carbon atom appeared at δ 166.1 ppm.

The proposed mechanism for the above reaction is given in Scheme 7.

Spectroscopic studies:

The UV spectra of the diazonium coupling products of compounds **6–13** indicate that they have an azo structure. Most of the dyes show two absorption bands between 230 and 390 nm. The slight differences in the maximum absorption wavelength (λ_{max}) can be attributed to the general solvent effect, which may alter the polarity of the absorbing system [37]. It has been observed that monophenylazo compounds exhibit

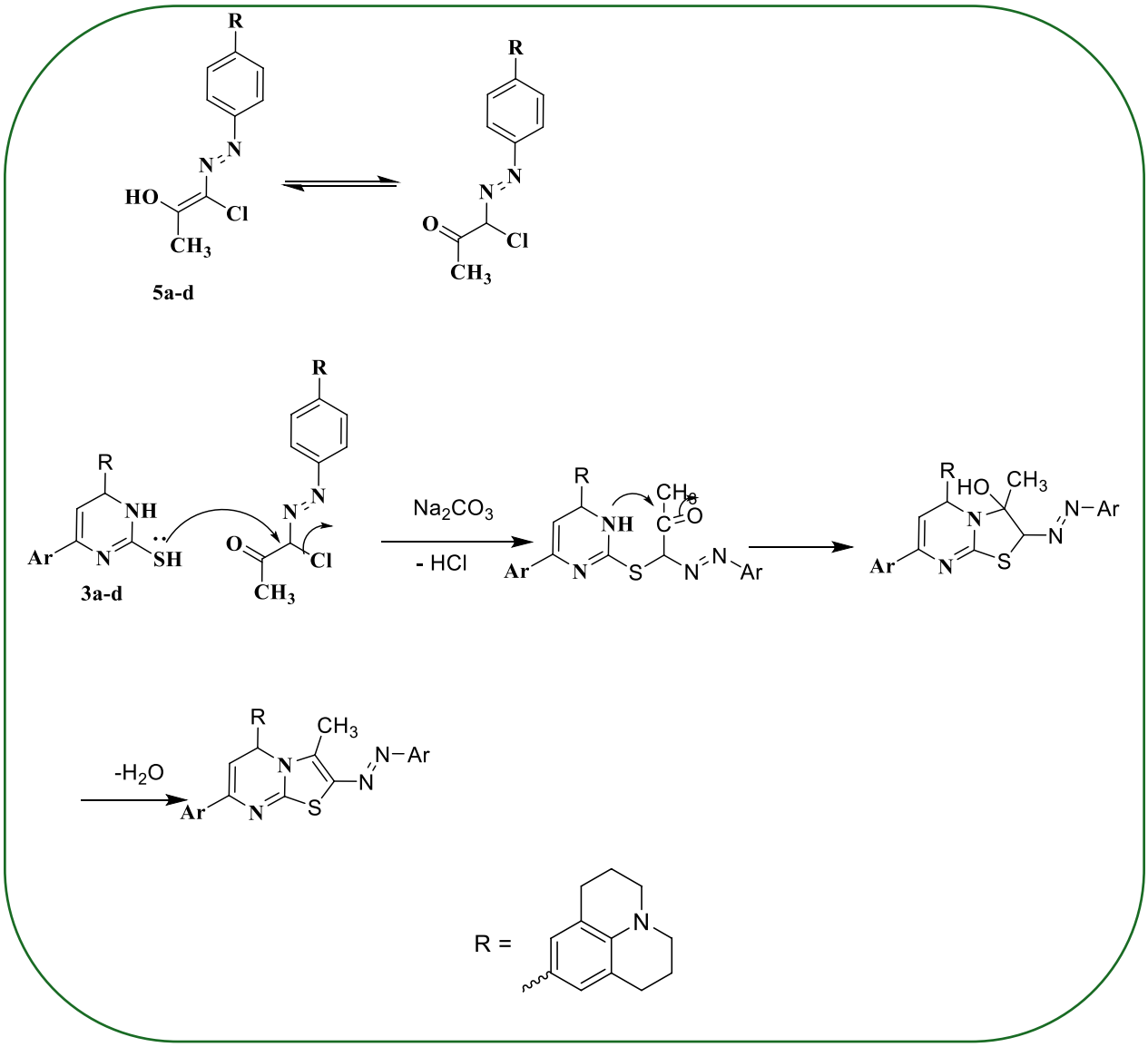

Scheme 5. Utility of hydrazonyl chloride **(5a-d)** in the synthesis of fused thiazolopyridopyrimidine derivatives **10–13**

different UV spectra compared to monophenylhydrazones. Azo compounds typically show two absorption bands due to n–π* and π–π* transitions [37]. In contrast, monophenylhydrazones display three strong absorption bands [37]. The UV spectra of compounds **6–13** cannot be explained by a hydrazo structure (Fig. 2).

The IR spectra of compounds **3a-d** generally exhibited absorption bands in the range of ν 3300–3250 cm^{-1}, corresponding to NH stretching, while the thione group showed an absorption band around ν 1300 cm^{-1}. In contrast, compounds **4a-d** displayed an NH absorption band at approximately ν 3200–3180 cm^{-1}, along with a carbonyl group absorption band near ν 1380 cm^{-1} and a thione group band around ν 1330 cm^{-1} (Fig. 3).

Moreover, the IR spectra of compounds **6–13**, in general, showed the appearance of an -N =N- functional group around ν 1580 cm^{-1} (Fig. 4).

A mass spectroscopic study of the newly synthesized compounds revealed a lack of literature on these derivatives, prompting an investigation into their fragmentation pathways. To date, no reports have been made on these compounds. In such structures, the initial charge is typically localized on nitrogen, oxygen, or the aromatic ring. For compounds **6–13**, the spectra generally showed

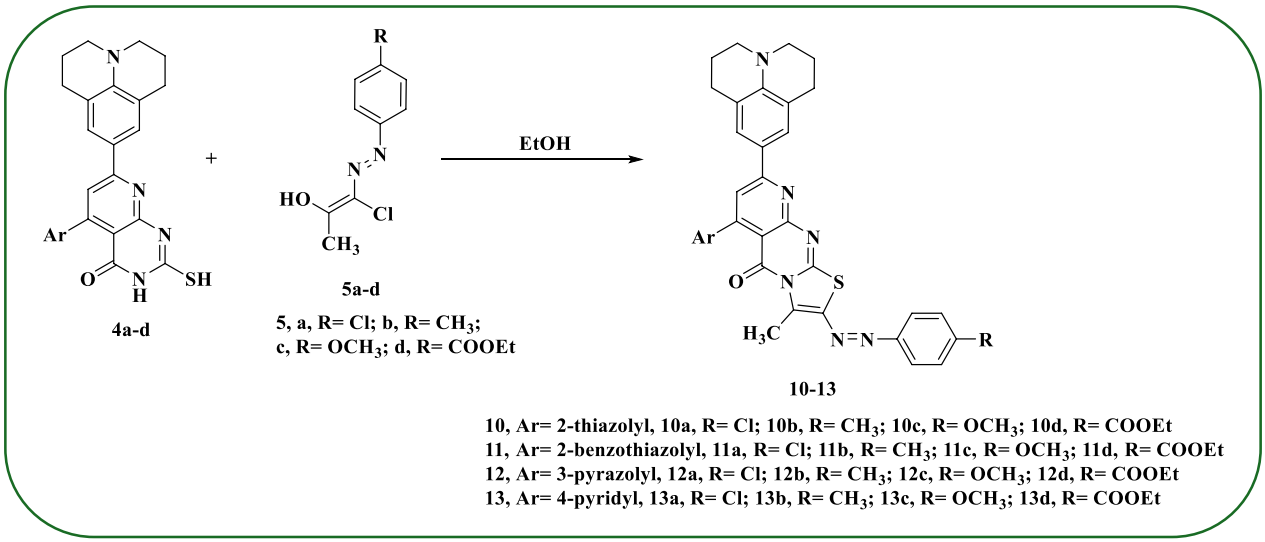

Scheme 6. The proposed mechanism for the synthesis of **6–9**

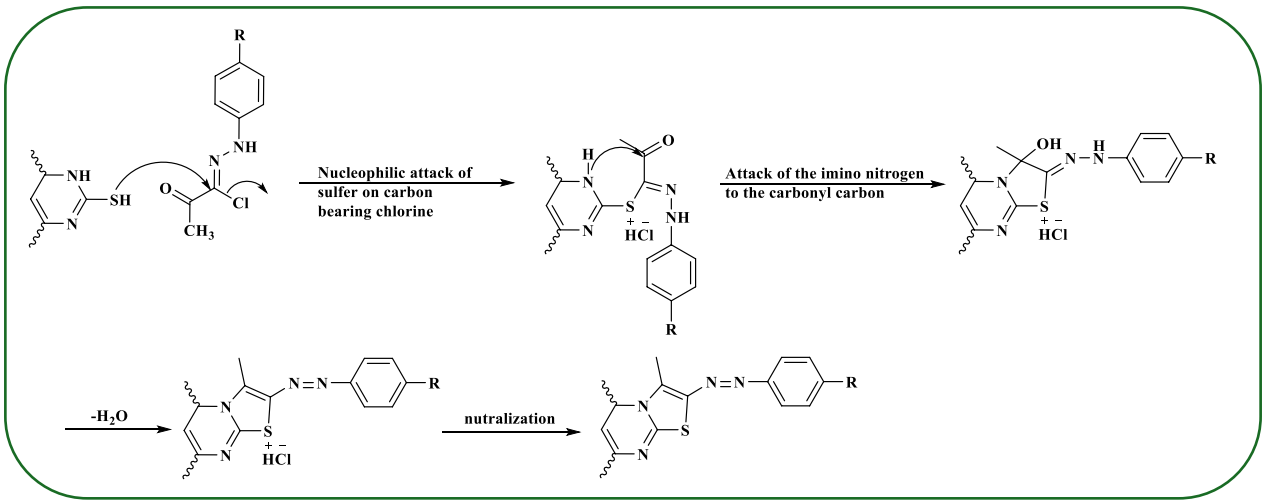

Scheme 7. The proposed mechanism for the above reaction

peaks corresponding to the loss of 104 mass units from the molecular ion, attributed to the elimination of a $C_6H_4N_2$ fragment. Additionally, a prominent base peak at 172 mass units was observed, corresponding to the decomposition of the julolidine moiety (Fig. 5).

Regarding to ^{1}H- and ^{13}C-NMR (*c.f.* results and discussion, experimental, and supplementary files.

Antimicrobial activity

Forty novel thiazolopyrimidines were synthesized and subjected to in vitro antibacterial screening against Gram-positive *S. aureus*, Gram-negative *E. coli*, and fungal species *C. albicans*. The detailed activity results (MIC values and inhibition zones) are presented in Table 1. Some of the synthesized novel thiazolopyrimidine derivatives exhibited varying levels of antimicrobial activity against the test microorganisms. Based on these data in Table 1, compounds **11a**, **11b**, **7a**, and **7b** were identified as the most active candidates and subsequently selected for molecular docking analysis against PDB: 1aj6. Compound **11a** exhibited the maximum inhibition zones (62 ± 1.0), (47 ± 0.5), and (50 ± 0.6), compound **11b** (61 ± 1.2), (46 ± 1.0), and (48 ± 0.5), compound **7a** (61 ± 1.1), (42 ± 0.6), and (46 ± 0.5), and compound **7b** (60 ± 1.1), (41 ± 0.6), and (47 ± 0.1) mm as well as, the MIC value of compound **11a** (5.9, 47.3, and 23.6 µM), compound **11b** (6.1, 48.8, and 24.4 µM), compound **7a** (6.5, 105.0, and 26.2 µM), and **7b**

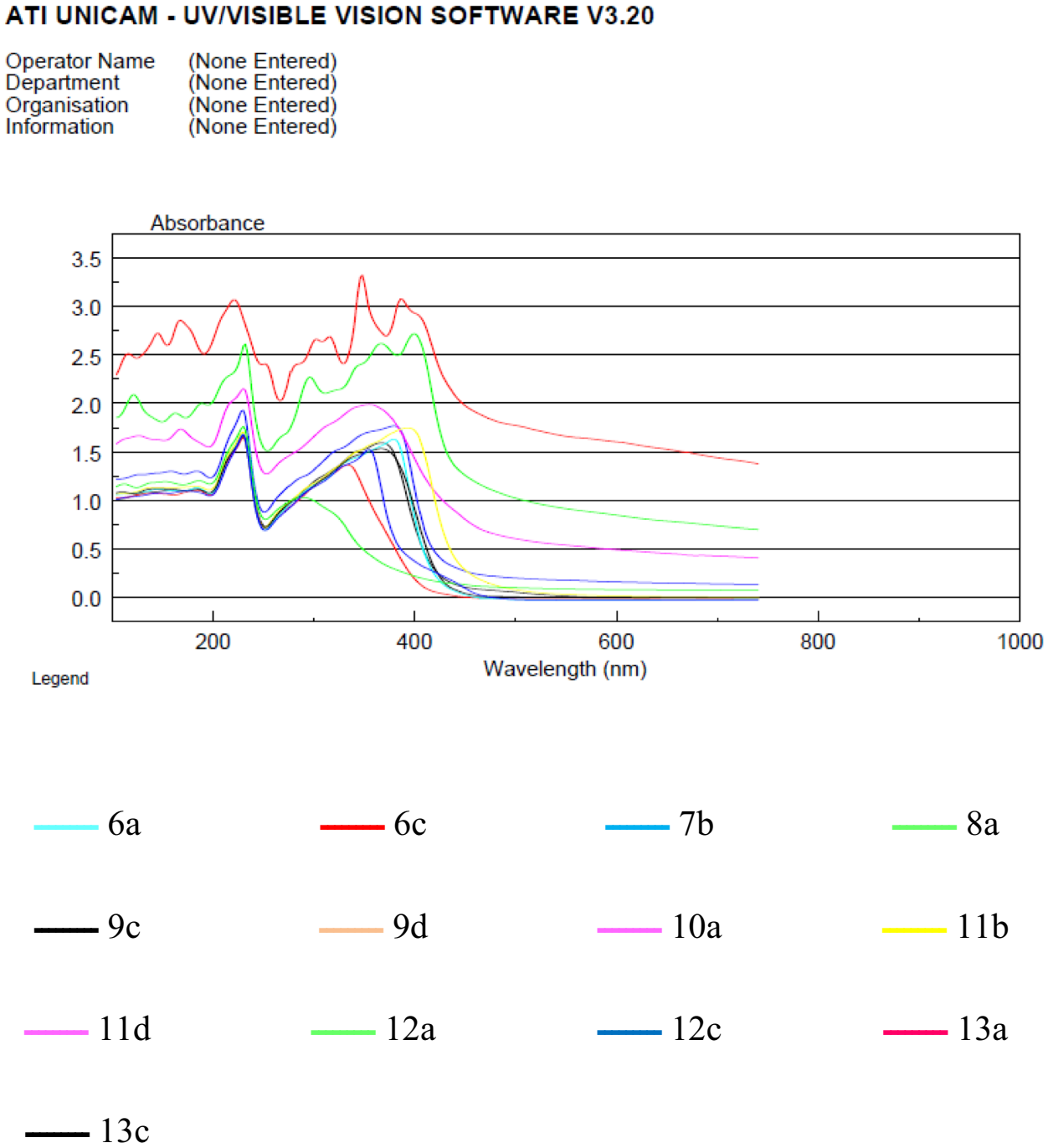

Fig. 2 Ultraviolet spectra of some selected compounds

(6.8, 217.5, and 27.1 µM) against *S. aureus*, *E. coli*, and C. *albicans*, respectively as compared to the reference drug. In addition to, thiazolopyrimidine derivatives **6a**, **7c**, **10a**, and **11c** exhibited very strong antibacterial activities, while compounds **6b-d**, **7 d**, **8a**, **9a-d**, **10b-d**, **11 d**, **12a-c**, and **13a-d** exhibited moderate activities against all the tested bacterial strains. The other rest of the compound displayed weak antibacterial activities against the tested bacterial strains. All tested thiazolopyrimidine derivatives showed weak activity against

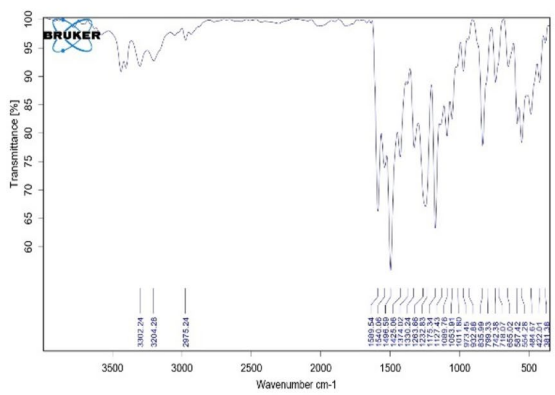

3b

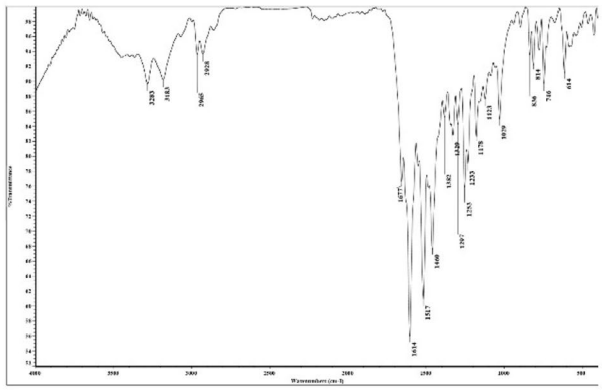

4b

Fig. 3 IR spectra of compounds **3b** and **4b**

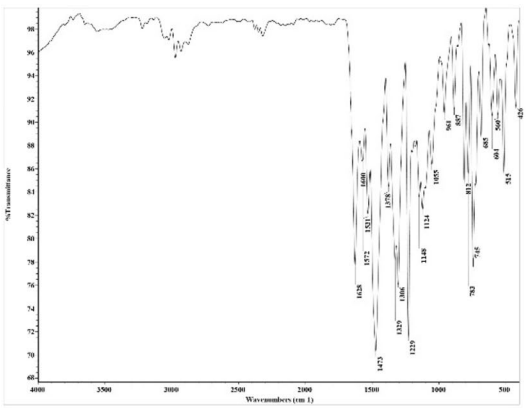

6a

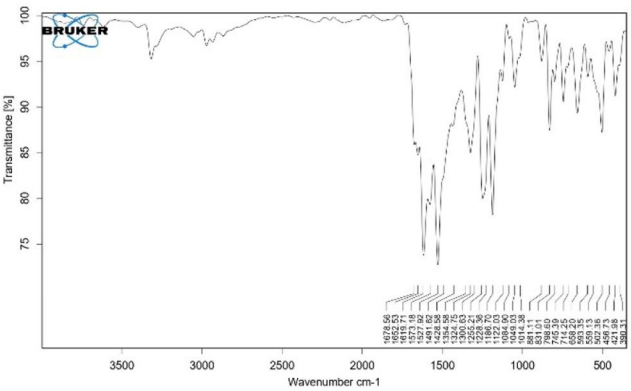

10a

Fig. 4 IR spectra of compounds **6a** and **10a**

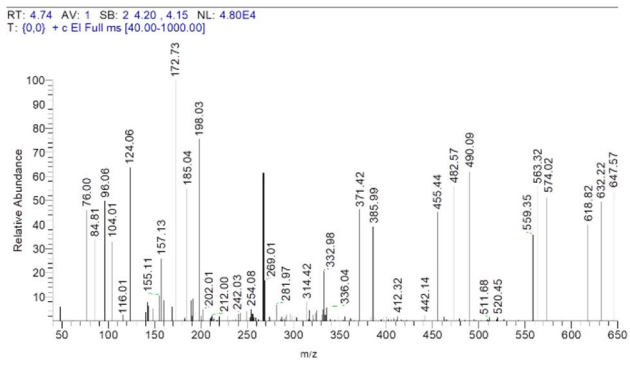

10d

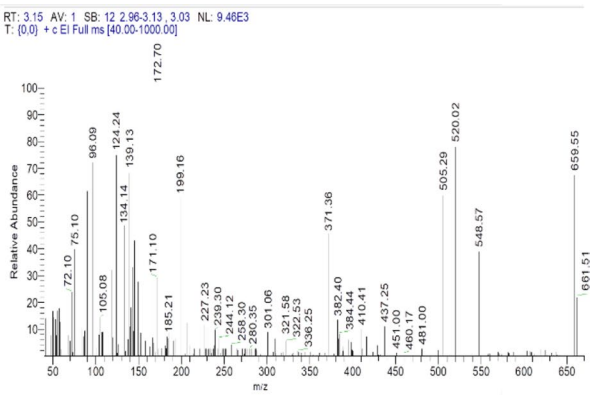

11a

Fig. 5 Mass spectra of compounds **10 d** and **11a**

Table 1 The antimicrobial activity of all newly synthesized compounds

Compound No	MIC (μM) and Inhibition Zone (mm)		
	Gram-positive bacteria	***Gram-negative bacteria***	***Fungi***
	S. aureus	***E. coli***	***C. albicans***
3a	678.4 (27 ± 0.5)	1356.8 (20 ± 0.5)	2713.5 (14 ± 0.5)
3b	597.2 (25 ± 1.0)	2389.0 (14 ± 0.1)	2389.0 (15 ± 0.1)
3c	1422.6 (20 ± 0.5)	2845.2 (13 ± 0.5)	2845.2 (13 ± 0.5)
3 d	689.6 (27 ± 0.5)	2758.6 (13 ± 0.5)	2758.6 (14 ± 0.6)
4a	288.3 (37 ± 0.5)	1153.3 (22 ± 0.5)	2306.5 (14 ± 0.5)
4b	258.5 (35 ± 0.5)	1033.9 (20 ± 0.1)	2067.8 (13 ± 0.5)
4c	600.2 (28 ± 0.5)	2400.9 (13 ± 0.5)	2400.9 (15 ± 0.1)
4 d	293.0 (37 ± 1.0)	2344.4 (13 ± 0.5)	2344.4 (14 ± 0.5)
6a	14.3 (53 ± 0.5)	57.3 (44 ± 0.5)	458.6 (27 ± 0.5)
6b	59.5 (48 ± 1.0)	119.1 (40 ± 0.5)	476.4 (30 ± 0.1)
6c	57.8 (47 ± 0.5)	115.6 (43 ± 0.6)	462.4 (29 ± 0.5)
6 d	107.3 (44 ± 0.5)	214.5 (36 ± 0.5)	858.0 (21 ± 0.1)
7a	6.5 (61 ± 1.1)	105.0 (42 ± 0.6)	26.2 (46 ± 0.5)
7b	6.8 (60 ± 1.1)	217.4 (41 ± 0.6)	27.1 (47 ± 0.1)
7c	13.2 (57 ± 0.5)	211.6 (40 ± 0.5)	105.8 (35 ± 0.5)
7 d	24.6 (51 ± 0.5)	197.5 (38 ± 1.0)	98.8 (41 ± 0.5)
8a	118.3 (42 ± 0.5)	946.8 (20 ± 0.5)	946.8 (19 ± 0.1)
8b	264.2 (37 ± 1.0)	1969.8 (13 ± 0.5)	1969.8 (14 ± 0.5)
8c	238.7 (38 ± 0.5)	1909.6 (14 ± 0.5)	1909.6 (13 ± 0.1)
8 d	441.9 (25 ± 0.5)	1767.7 (14 ± 0.1)	1767.7 (14 ± 0.6)
9a	57.9 (42 ± 0.5)	463.7 (23 ± 0.5)	1854.9 (15 ± 0.5)
9b	60.2 (46 ± 0.5)	963.9 (19 ± 1.0)	1927.9 (13 ± 0.5)
9c	116.9 (43 ± 1.0)	1870.2 (14 ± 0.5)	935.1 (19 ± 0.6)
9 d	108.4 (43 ± 0.5)	866.9 (21 ± 0.5)	1733.9 (14 ± 0.5)
10a	12.8 (53 ± 0.5)	409.7 (25 ± 1.0)	409.7 (26 ± 0.5)
10b	26.5 (52 ± 1.0)	423.9 (30 ± 0.5)	423.9 (30 ± 0.6)
10c	51.6 (48 ± 0.5)	825.4 (27 ± 0.5)	825.4 (18 ± 0.1)
10 d	48.2 (46 ± 1.0)	385.9 (21 ± 0.5)	771.8 (20 ± 0.5)
11a	5.9 (62 ± 1.0)	47.3 (47 ± 0.5)	23.6 (50 ± 0.6)
11b	6.1 (61 ± 1.2)	48.8 (46 ± 1.0)	24.4 (48 ± 0.5)
11c	11.9 (58 ± 1.0)	95.3 (42 ± 0.6)	47.6 (40 ± 0.5)
11 d	22.4 (50 ± 1.0)	89.6 (41 ± 0.5)	89.6 (40 ± 0.6)
12a	105.4 (40 ± 1.0)	843.0 (20 ± 0.5)	421.5 (31 ± 0.5)
12b	109.1 (40 ± 0.5)	873.0 (21 ± 0.1)	1746.1 (15 ± 0.6)
12c	106.2 (42 ± 0.5)	1698.7 (14 ± 0.5)	424.7 (26 ± 0.6)

Table 1 (continued)

Compound No	MIC (μM) and Inhibition Zone (mm)		
	Gram-positive bacteria	*Gram-negative bacteria*	*Fungi*
	S. aureus	*E. coli*	*C. albicans*
12 d	198.2 (36 ± 0.5)	1585.4 (13 ± 0.5)	1585.4 (13 ± 0.6)
13a	25.8 (52 ± 0.5)	209.9 (36 ± 0.5)	1655.2 (14 ± 0.1)
13b	53.5 (46 ± 1.0)	428.3 (30 ± 0.6)	856.6 (20 ± 0.5)
13c	104.2 (33 ± 0.5)	833.7 (22 ± 0.5)	833.7 (18 ± 0.1)
13 d	97.4 (44 ± 0.5)	389.5 (30 ± 0.5)	389.5 (27 ± 0.5)
Gentamicin	–	130.9 (28 ± 0.5)	–
Ampicillin	178.9 (22 ± 0.1)	–	–
Cycloheximide	–	–	111.1 (42 ± 0.5)

C. albicans fungal strains except compounds **7a**, **7b**, **11a**, and **11b** exhibited good activity.

Structure–Activity relationship

From the results in Table 1, the antimicrobial activity of compounds **3** and **4** are influenced by several factors, including structural features, electronic distribution, and steric effect. Compound **3** has a dihydropyrimidine-thione core, while compound **4** has a dihydropyrido-pyrimidin-one core. The latter structure (compound **4**) might offer greater rigidity and planarity, which can influence binding to microbial targets. Moreover, both compounds feature sulfur-containing groups (thione and thioxo). Thione and thioxo groups are often involved in bioactivity due to their ability to interact with various biological targets through hydrogen bonding or coordination with metal ions in enzymes, as reported in several studies [38]. In addition, the position and nature of the aryl and tetrahydropyridoquinoline substituents can affect lipophilicity and the ability to traverse biological membranes, impacting antimicrobial activity. Compound **4** positions these groups at 5 and 7 respectively, which may lead to a more favorable spatial arrangement for interactions with microbial targets compared to compound **3**. The electronic distribution influenced by the substitution pattern may alter the ability of the compound to engage in electronic interactions (e.g., π-π stacking) with microbial DNA or proteins. The structural differences suggest that compound 4 could have an enhanced electronic profile due to the extended conjugation system offered by the pyrido[2,3-d] pyrimidinone core and consequently, it will be more active as an antimicrobial agent than compound **3**.

To analyze the results of antibacterial activity displayed by compounds **6–9**, and similarly **10–13**, in Table 1, the benzothiazolyl group in compounds **7** and **11** provides increased rigidity, aromaticity, and potential electronic interactions, making it likely the most active due to enhanced binding affinity and overall antimicrobial potential.

The thiazolyl group in compounds **6** and **10** offers good electronic properties and lipophilicity, but not as much aromatic rigidity as the benzothiazolyl group in compounds **7** and **11**. Thus, it is likely slightly less active than compounds **7** and **11**. In compounds **8** and **12**, the pyrazolyl group offers additional hydrogen bonding potential but lacks the same level of aromaticity and electronic interaction capacity compared to the benzothiazolyl, thiazolyl, and pyridinyl groups, likely making it the least active. On the other hand, the pyridinyl group in compounds **9**, and **13** can enhance interactions with microbial targets through aromaticity and hydrogen bonding but may be less effective than the benzothiazolyl and thiazolyl groups in compounds **7**, **11**, **6**, and **10**.

From the results in Table 1, It was noticed that the 4-chlorophenyl group as a substituent in derivative **(a)** is an electron-withdrawing group enhancing lipophilicity and potential interactions with microbial targets, making it likely the most active. The *p*-tolyl substituent group in derivative **(b)** is less electron-withdrawing than chlorophenyl group, likely resulting in slightly lower activity compared to a substituent **(a)**. In addition, the *p*-methoxy substituent group in derivative **(c)** is an electron-donating group, potentially decreasing antimicrobial activity by increasing electron density and reducing interaction efficiency with microbial targets. Finally, the bulky ester substituent group in derivative **(d)** may hinder interaction with microbial targets due to steric hindrance, likely

Table 2 Docking results of the selected derivatives with a high score of MIC

Der	S (Kcal/mol)	RMSD	ligand bindings with the amino-acid residues	Types of Interactions	Distance (Å)
7a	− 6.7395	1.4639	S 21 of thiazole ring with Asn 46	H-donor	3.68
7b	− 7.0691	1.9989	C 19 of pyrimidine ring with Glu 42	H-donor	3.41
			Thiazole-ring with Asn 46	Pi-H	4.23
11a	− 7.2219	1.9440	Phenyl of quinoline ring with Gly 102	Pi-H	4.02
			Phenyl of quinoline ring with Lys 103	Pi-H	3.93
11b	− 7.3404	1.9479	Phenyl of quinoline ring with Gly 102	Pi-H	4.02
			Phenyl of quinoline ring with Lys 103	Pi-H	3.91

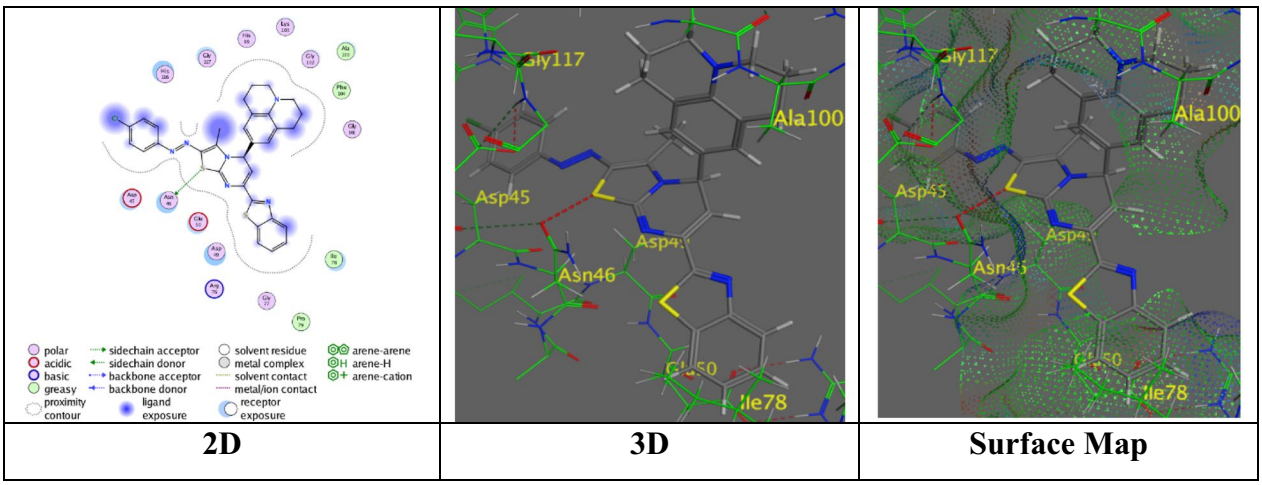

Fig. 6 Interaction images between derivative **7a** with (PDB: 1aj6)

making it the least active substituent. The overall conclusion compounds **10–13** which contain thiazolopyridipyrimidine derivatives are more active than compounds **6–9** which contain thiazolopyrimidine derivatives against the tested microbes.

Based on the above structural analysis, the highest activity compounds **11a**, and **11b** are due to the presence of the extended conjugation system offered by the pyridopyrimidine system and the presence of benzothiazole ring. Similarly, the high reactivity of compounds **7a** and **7b** is also due to the presence of benzothiazole moiety.

Molecular docking study

The binding affinities of the derivatives were evaluated using the London dG scoring function, and the docking scores (ΔG) are reported in kcal/mol. Key interactions with residues such as Asn 46, Glu 42, Gly 102, and Lys 103 were analyzed, including both of H-donor and π-H bindings (Table 2). Derivative **7a** exhibited a moderate docking score = − 6.7395 kcal/mol with an RMSD of 1.4639 Å. The ligand binding study showed that the sulfur atom (S 21) in the thiazole ring donates a hydrogen atom to the Asn 46 residue, which is 3.68 Å away (Fig. 6). While derivative **7b** displayed a higher docking score = − 7.0691 kcal/mol and an RMSD of 1.9989 Å. The interactions involved the carbon atom (C 19) of the pyrimidine ring with Glu 42 through a hydrogen donor interaction at 3.41 Å, and the thiazole ring with Asn 46 through a pi-hydrogen (Pi-H) interaction at 4.23 Å (Fig. 7). These interactions indicate a slightly better binding affinity, and a more complex interaction profile compared to **7a**. Meanwhile, derivative **11a** demonstrated a docking score = − 7.2219 kcal/mol with an RMSD of 1.9440 Å. The phenyl group of the quinoline ring made Pi-H interactions with residues Gly 102 and Lys 103, which were 4.02 Å and 3.93 Å apart, respectively (Fig. 8). This suggests a significant binding affinity with dual interaction sites, enhancing its potential efficacy. Moreover, derivative **11b** showed the best docking score among the derivatives at − 7.3404 kcal/mol with an RMSD of 1.9479 Å. Like **11a**, it exhibited Pi-H interactions with Gly 102 and Lys 103 at distances of 4.02 Å and 3.91 Å, respectively (Fig. 9). The small increase in the docking score and interaction

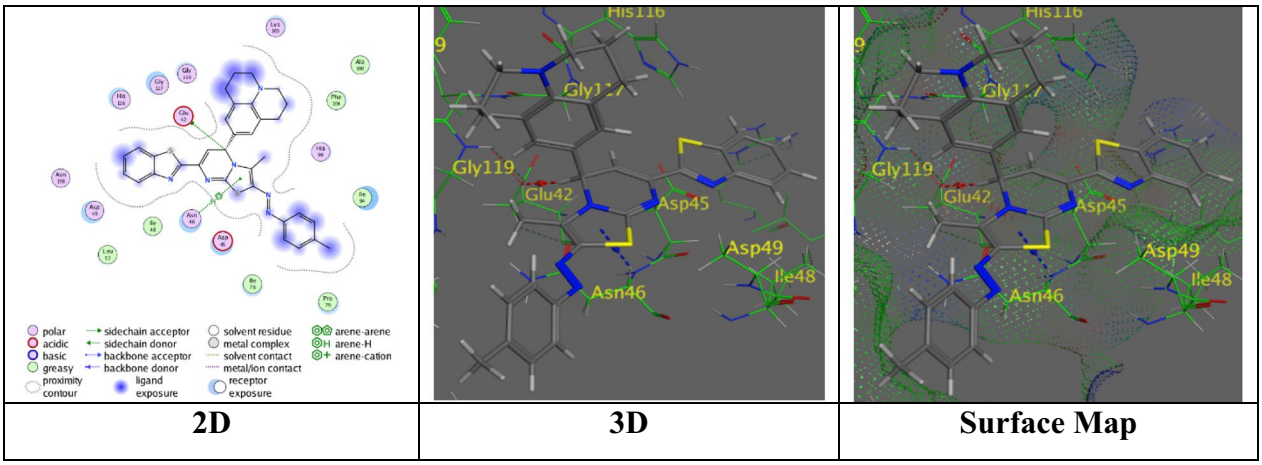

Fig. 7 Interaction images between derivative **7b** with (PDB: 1aj6)

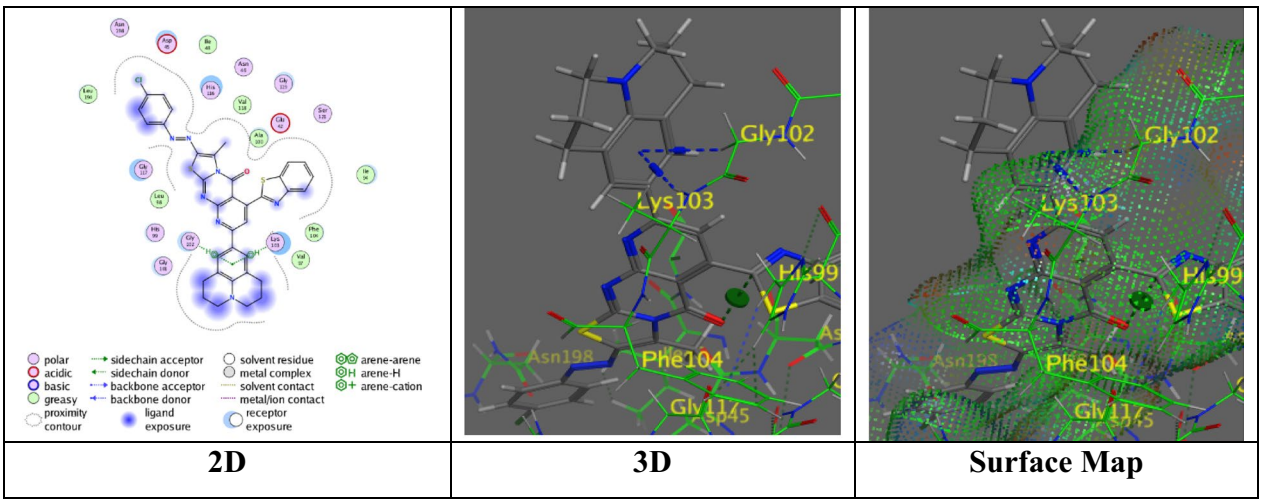

Fig. 8 Interaction images between derivative **11a** with (PDB: 1aj6)

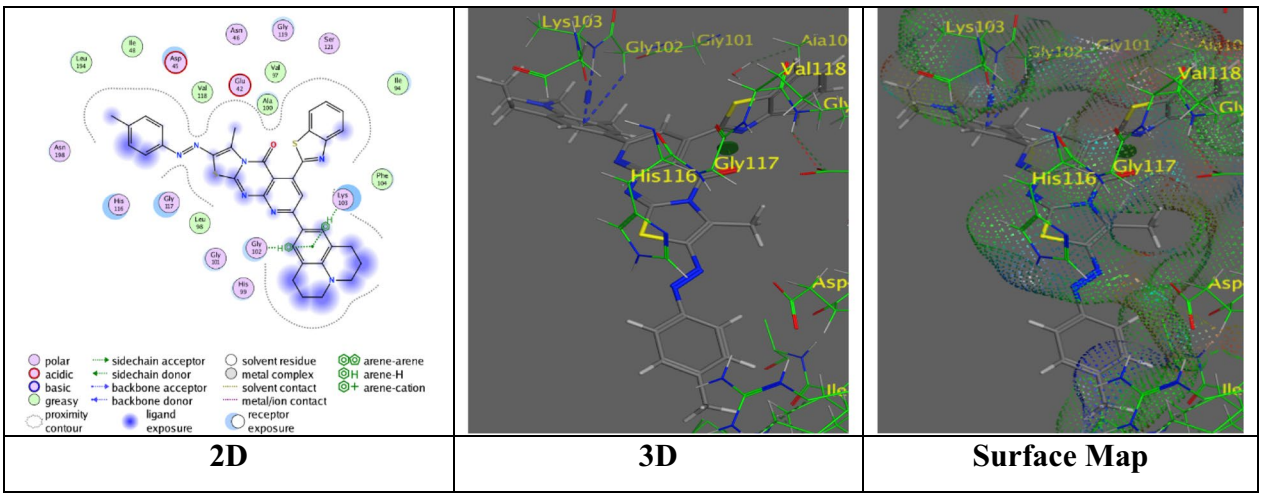

Fig. 9 Interaction images between derivative **11b** with (PDB: 1aj6)

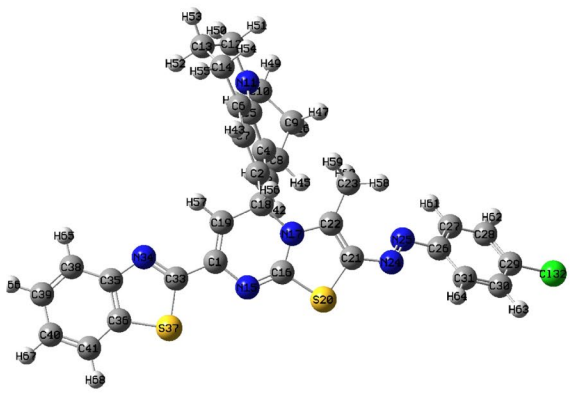

7a; Electronic Energy = -2820.144 Hartree; Dipole Moment = 6.6912595 Debye

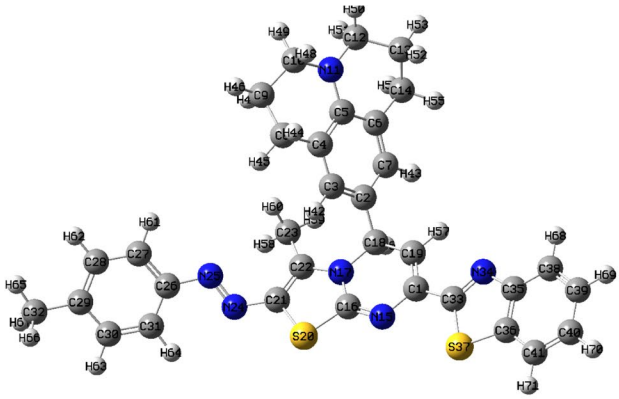

7b; Electronic Energy = -2399.8784 Hartree; Dipole Moment = 7.1048577 Debye

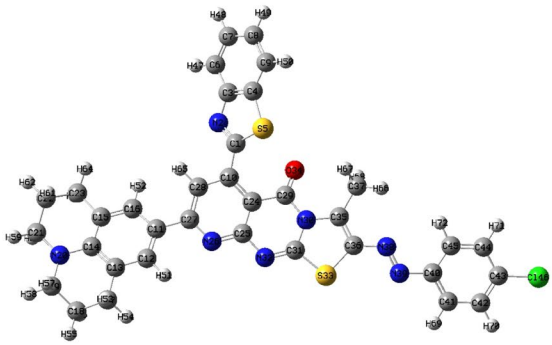

11a; Electronic Energy = -3063.8131 Hartree; Dipole Moment = 3.9389481 Debye

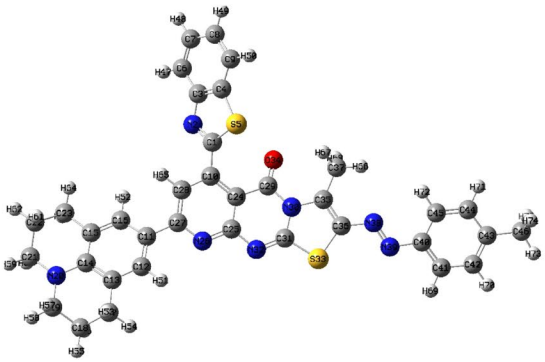

11b; Electronic Energy = -2643.5514 Hartree; Dipole Moment = 1.9057645 Debye

Fig. 10 The optimized structures of selected compounds

distances shows a better binding profile, which makes it more likely that it could be a prime derivative.

Molecular modelling

Structural optimization

Four selected conformers (**7a**, **7b**, **11a** and **11b**) were studied to elucidate their structures as an example as well as to investigate the relation between their structures and their notable priority in biological activity. The structures of these compounds were built on Gaussian 09 software was applied under DFT/B3LYP method by using 6-31G* basis set (Fig. 10). The obtained files (log, chk and fchk) were visualized in the program screen to obtain the HOMO, LUMO (Fig. 11) as well as the MEP maps (Fig. 12). The formation energy of four conformers were calculated (Fig. 10) and the values reflect their stability. As well as the dipole moment values were estimated and the reduced values of these compounds particularly the **11a** and **11b** conformers support their high ability of lipophilicity inside the cell lipid [39, 40].

The physical features

The HOMO and LUMO frontiers patterns (Fig. 11) were established via a cube counter on the molecular surface and their energy values were computed to evaluate the energy gap in between ($\Delta E = E_{LUMO}$-E_{HOMO}). The band gap values − 0.08535, − 0.09034, − 0.07642 and − 0.08292 eV, for **7a**, **7b**, **11a** and **11b** respectively. The values appeared small which clarfay the ease of electronic transitions inside these conformers which kake these compounds active towards

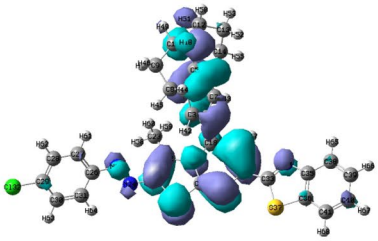

7a; HOMO = -0.17858 eV

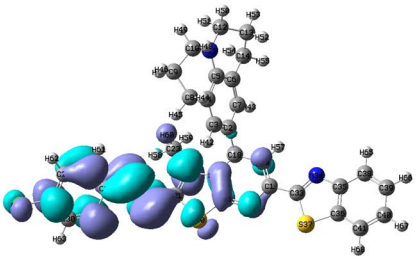

7a; LUMO = -0.09323 eV

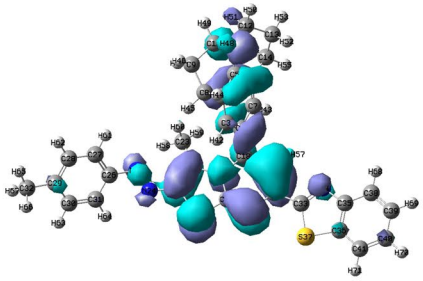

7b; HOMO = -0.17423 eV

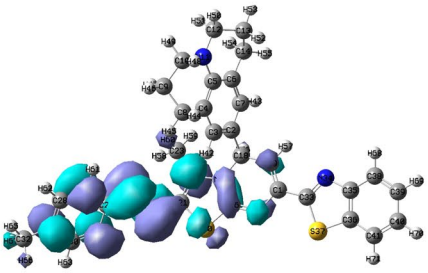

7b; LUMO = -0.08389 eV

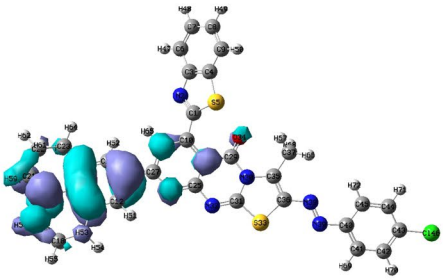

11a; HOMO = -0.18098 eV

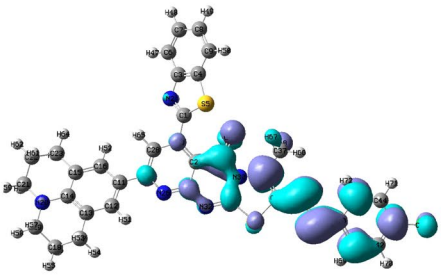

11a; LUMO = -0.10456 eV

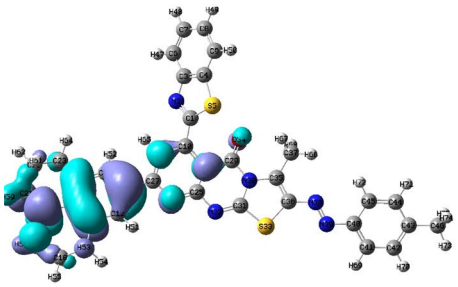

11b; HOMO = -0.17877 eV

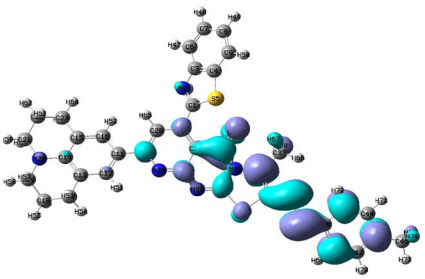

11b; LUMO = -0.09585 eV

Fig. 11 The frontier orbitals for selected compounds

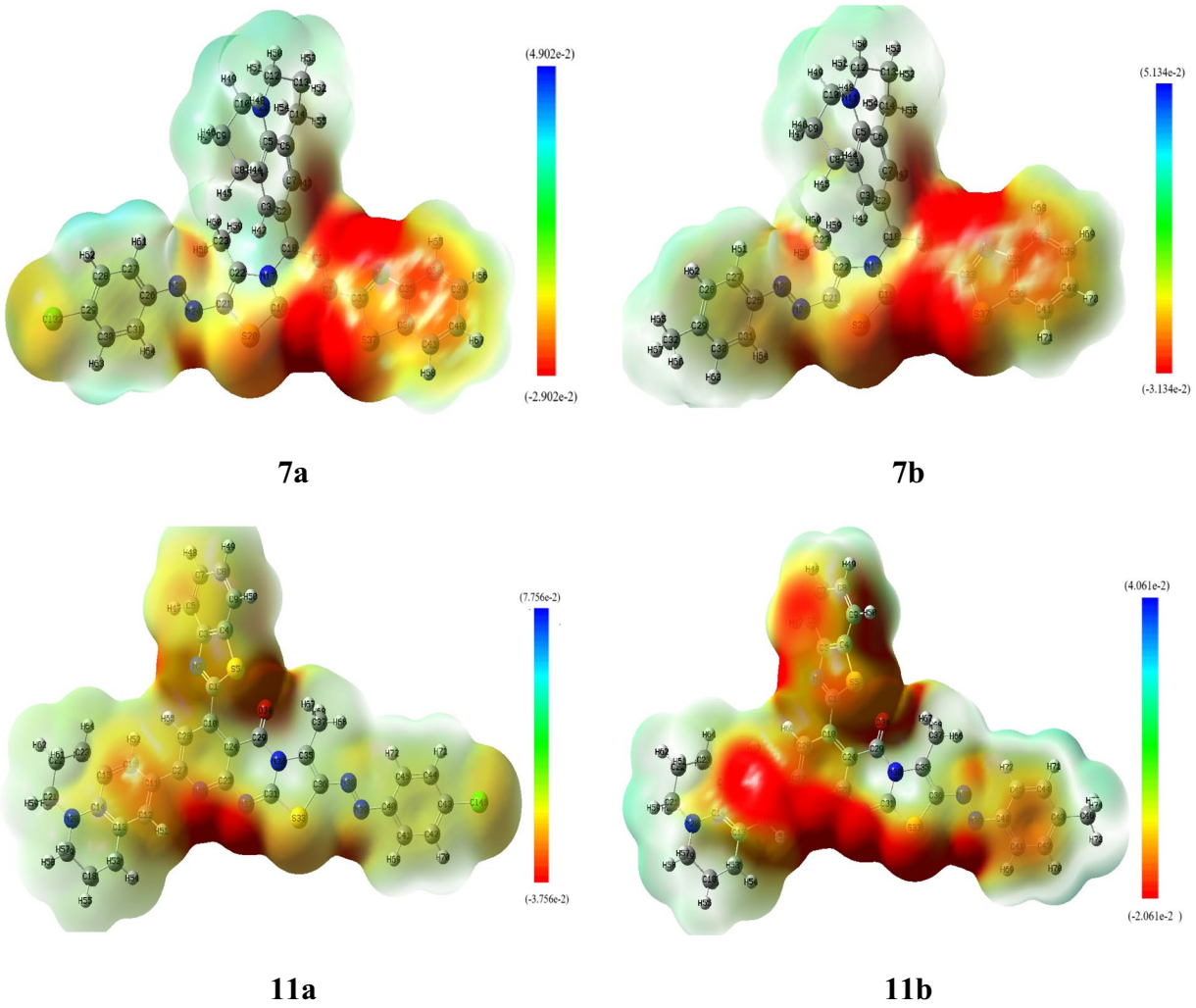

Fig. 12 Electrostatic potential maps (MEP) of the optimized structures

interaction incide the microbial cells and interact with biological systems [39, 41]. The electrostatic potential maps (MEP) (Fig. 12) were also established to assess the electron cloud distribution over the whole functional groups. Then we could differentiate between the nucleophilic, electrophilic, and neutral zones which are depicted by red, blue, and green colors respectively. Most functional groups exhibited their nucleophilicity as appeared in four MEP maps, the red zone is predominant and this is promising feature during interaction inside microbial cells [42, 43].

Experiment

Materials and methods

All starting materials and reagents, including julolidine-9-carbaldehyde, aryl acetyl derivatives, 6-amino-2-thiouracil, and hydrazonyl chloride derivatives **5a–d** were obtained as follows:

2-Acetyl thiazole (purity 99%) was purchased from Alfa Aesar company, b.p. 89–91 °C/12 mm.

2-Acetyl benzothiazole (yield 65%) was prepared according to previously reported work [44], m.p. 103–105 °C [Lit 105–107 °C [44]].

3-acetyl pyrazole (yield 76%) was prepared according to previously reported work [45], m.p. 95–97 °C [Lit 96–97 °C [45]].

4-Acetyl pyridine (purity 97%) was purchased from Aldrich company, b.p. 212–214 °C, m.p. 13–16 °C.

Julolidine-9-carbaldahyde was obtained from Tokyo Chemical Industry (purity 98%),

m.p. 83 °C.

6-amino-2-thiouracil (yield 70%) was prepared according to previously reported work [46], m.p. < 300 °C [Lit 330–340 °C [46]].

Compound 5a: (yield 70%) was prepared according to previously reported work [34], m.p. 176–178 °C [Lit 180 °C [34]].

Compound 5b: (yield 75%) was prepared according to previously reported work [34], m.p. 140–142 °C [Lit 142 °C [34]].

Compound 5c: (yield 76%) was prepared according to previously reported work [47], m.p. 118–120 °C [Lit 120–122 °C [47]].

Compound 5 d: (yield 73%) was prepared according to previously reported work [35], m.p. 165–167 °C [Lit 167–169 °C [35]].

Synthesis of chalcones derivatives (2a-d)

General procedure:

An equimolar amount of julolidine-9-carbaldahyde (0.2 g, 1 mmol) and the appropriate aryl acetyl derivatives **1a-d** (1 mmol) were stirred at room temperature overnight in alcoholic KOH (10%). Diluted HCl was used to neutralize the reaction mixture after its cooling in an ice bath to give the corresponding chalcones derivatives **(2a-d)**.

3-(2,3,6,7-Tetrahydro-1*H*,5*H*-pyrido[3,2,1-*ij*]quinoline-9-yl)−1-(thiazol-2-yl)prop-2-en-1-one (2a)

Yield, 81%; m.p. 167–169 °C; IR (KBr): ν_{max}, cm^{-1}: 1660 (C =O), 1595 (C =C) (Figure S1); ^{1}H-NMR (DMSO-d_6) δ ppm: 1.93 (m, 4H, 2CH_2), 2.75 (t, 4H, 2CH_2), 3.45 (t, 4H, 2CH_2), 6.79 (d, 1H, *J=15* Hz, olefinic-CH), 6.97 (s, 2H, Ar–H), 7.69 (d, 1H, *J=15* Hz, olefinic-CH), 7.80 (d, 1H, *J=8* Hz, thiazole-CH), 7.99 (d, 1H, *J=8* Hz, thiazole-CH) (Figure S2); ^{13}C-NMR (DMSO-d_6) δ ppm: 22.5 (2 C), 28.0 (2 C), 51.5 (2 C), 121.5, 122.4 (2 C), 123.6 (2 C), 125.0, 132.6, 142.5, 143.7, 145.6, 164.3, 187.1. MS (m/z, %): 310 (M^+, 55). Anal. Calced for $C_{18}H_{18}N_2OS$ (310.42): C, 69.65; H, 5.85; N, 9.02%. Found: C, 69.59; H, 5.76; N, 8.93%.

1-(Benzo[d]thiazol-2-yl)−3-(2,3,6,7-tetrahydro-1*H*,5*H*-pyrido[3,2,1-*ij*]quinoline-9-yl)prop-2-en-1-one (2b):

Yield, 77%; m.p. 216–218 °C; IR (KBr): ν_{max}, cm^{-1}: 1665 (C =O), 1592 (C =C) (Figure S3); ^{1}H-NMR (DMSO-d_6) δ ppm: 1.80 (m, 4H, 2CH_2), 2.75 (t, 4H, 2CH_2), 3.50 (t, 4H, 2CH_2), 6.70 (d, 1H, *J=15* Hz, olefinic-CH), 6.95 (s, 2H, Ar–H), 7.50–8.02 (m, 5H, 4 Ar–H + olefinic-CH); ^{13}C-NMR (DMSO-d_6) δ ppm: 22.5 (2 C), 28.7 (2 C), 51.4 (2 C), 121.2 (2 C), 122.1 (2 C), 123.1 (2 C), 124.8 (2 C), 126.0 (2 C), 136.0, 142.5, 145.9, 153.0, 160.1, 188.0 (Figure S4). MS (m/z, %): 360 (M^+, 60). Anal. Calced for $C_{22}H_{20}N_2OS$ (360.48): C, 73.30; H, 5.59; N, 7.77%. Found: C, 73.26; H, 5.51; N, 7.69%.

1-(1*H*-pyrazol-3-yl)−3-(2,3,6,7-tetrahydro-1*H*,5*H*-pyrido[3,2,1-*ij*]quinoline-9-yl)prop-2-en-1-one (2c):

Yield, 80%; m.p. 187–189 °C; IR (KBr): ν_{max}, cm^{-1}: 3234 (NH), 1660 (C =O), 1595 (C =C) (Figure S5); ^{1}H-NMR (DMSO-d_6) δ ppm: 1.84 (m, 4H, 2CH_2), 2.71 (t, 4H, 2CH_2), 3.55 (t, 4H, 2CH_2), 6.50 (d, 1H, *J=9* Hz, pyrazole-CH), 6.85 (d, 1H, *J=14.5* Hz, olefinic-CH), 6.99 (s, 2H, Ar–H), 7.75 (d, 1H, *J=15* Hz, olefinic-CH), 7.90 (d, 1H, *J=9* Hz, pyrazole-CH), 12.63 (s, 1H, NH); ^{13}C-NMR (DMSO-d_6) δ ppm: 23.5 (2 C), 29.5 (2 C), 51.8 (2 C), 104.0, 121.6, 122.5 (2 C), 123.7 (2 C), 125.2, 131.9, 132.9, 143.1, 146.1, 188.1 **(Figure S6)**. MS (m/z, %): 293 (M^+, 65). Anal. Calced for $C_{18}H_{19}N_3O$ (293.37): C, 73.69; H, 6.53; N, 14.32%. Found: C, 73.60; H, 6.47; N, 14.29%.

1-(Pyridin-4-yl)−3-(2,3,6,7-tetrahydro-1*H*,5*H*-pyrido[3,2,1-*ij*]quinoline-9-yl)prop-2-en-1-one (2 d):

Yield, 83%; m.p. 172–174 °C; IR (KBr): ν_{max}, cm^{-1}: 1666 (C =O), 1601 (C =C); ^{1}H-NMR (DMSO-d_6) δ ppm: 1.91 (m, 4H, 2CH_2), 2.89 (t, 4H, 2CH_2), 3.50 (t, 4H, 2CH_2), 6.69 (d, 1H, *J=12* Hz, olefinic-CH), 7.02 (s, 2H, Ar–H), 7.77 (d, 1H, *J=12.5* Hz, olefinic-CH), 8.00 (d, 2H, *J=9* Hz, Ar–H), 8.90 (d, 2H, *J=9* Hz, Ar–H) (Figure S7); ^{13}C-NMR (DMSO-d_6) δ ppm: 23.5 (2 C), 29.5 (2 C), 51.0 (2 C), 120.6, 121.8 (2 C), 122.7 (2 C), 124.2 (2 C), 125.3, 140.0, 143.7, 146.8, 151.8 (2 C), 189.9 (Figure S8). MS (m/z, %): 304 (M^+, 63). Anal. Calced for $C_{20}H_{20}N_2O$ (304.39): C, 78.92; H, 6.62; N, 9.20%. Found: C, 78.86; H, 6.57; N, 9.15%.

Synthesis of 3,4-dihydropyrimidine-2-thion derivatives (3a-d):

General procedure

Chalcones **2a-d** (5 mmol), potassium hydroxide (0.45 mg, 8 mmol), and thiourea (0.38 g, 5 mmol) were heated at reflux for five hours in absolute ethanol (20 mL). Following cooling, the reaction mixture was acidified by adding drops of diluted HCl, filtered off, and washed with water. Compounds **3a–d** was then obtained by recrystallizing the precipitated solid from ethanol.

4-(2,3,6,7-Tetrahydro-1*H*,5*H*-pyrido[3,2,1-*ij*]quinoline-9-yl)−6-(thiazol-2-yl)−3,4-dihydropyrimidine-2(1*H*)-thione (3a):

Yield, 78%; m.p. 210–212 °C; IR (KBr): ν_{max}, cm^{-1}: 3317, 3250 (2 NH), 1592 (C =C), 1324 (C =S) (Figure S9); ^{1}H-NMR (DMSO-d_6) δ ppm: 1.93 (m, 4H, 2CH_2), 2.80 (t, 4H, 2CH_2), 3.41 (t, 4H, 2CH_2), 4.60 (d, 1H, *J=9* Hz, pyrimidine-CH), 6.75 (d, 1H, *J=9* Hz, pyrimidine-CH), 6.95 (s, 2H, Ar–H), 7.54 (d, 1H, *J=8* Hz, thiazole-CH), 7.66 (d, 1H, *J=8* Hz, thiazole-CH), 9.78 (s, 1H, NH), 13.50 (s, 1H, NH); ^{13}C-NMR (DMSO-d_6) δ ppm: 21.9 (2 C), 27.9 (2 C), 50.8 (2 C), 61.8, 101.0, 121.8 (2 C), 126.0 (2 C), 132.0, 133.4, 140.0, 142.0, 148.4, 164.1, 174.5 (Figure S10). MS (m/z, %): 368 (M^+, 69), 284 (60), 196 (52), 172 (100), 122 (34), 112 (38), 102 (28), 84 (40), 74 (37), 70 (61), 57

(51) (Figure S11). Anal. Calced for $C_{19}H_{20}N_4S_2$ (368.52): C, 61.93; H, 5.47; N, 15.20%. Found: C, 61.85; H, 5.40; N, 15.15%.

6-(Benzo[d]thiazol-2-yl)−4-(2,3,6,7-tetrahydro-1*H*,5*H*-pyrido[3,2,1-*ij*]quinoline-9-yl)−3,4-dihydropyrimidine-2(1*H*)-thione (3b):

Yield, 77%; m.p. 244–246 °C; IR (KBr): ν_{max}, cm^{-1}: 3312, 3302 (2 NH), 1589 (C =C), 1330 (C =S) (Figure S12); ^{1}H-NMR (DMSO-d_6) δ ppm: 1.79 (m, 4H, 2CH_2), 2.90 (t, 4H, 2CH_2), 3.50 (t, 4H, 2CH_2), 4.64 (d, 1H, *J*=*9* Hz, pyrimidine-CH), 6.73 (d, 1H, *J*=*9* Hz, pyrimidine-CH), 7.05 (s, 2H, Ar–H), 7.50 (m, 2H, benzothiazole-CH), 8.05 (d, 1H, *J*=*9* Hz, benzothiazole-CH), 8.29 (d, 1H, *J*=*9* Hz, benzothiazole-CH), 9.68 (s, 1H, NH), 12.50 (s, 1H, NH) (Figure S13). MS (m/z, %): 418 (M^+, 68). Anal. Calced for $C_{23}H_{22}N_4S_2$ (418.58): C, 66.00; H, 5.30; N, 13.39%. Found: C, 65.93; H, 5.22; N, 13.30%.

6-(1*H*-pyrazol-3-yl)−4-(2,3,6,7-tetrahydro-1*H*,5*H*-pyrido[3,2,1-*ij*]quinoline-9-yl)−3,4-dihydropyrimidine-2(1*H*)-thione (3c):

Yield, 73%; m.p. 230–232 °C; IR (KBr): ν_{max}, cm^{-1}: 3319, 3250 (2 NH), 1600 (C =C), 1334 (C =S) (Figure S14); ^{1}H-NMR (DMSO-d_6) δ ppm: 1.75 (m, 4H, 2CH_2), 2.89 (t, 4H, 2CH_2), 3.49 (t, 4H, 2CH_2), 4.60 (d, 1H, *J*=*8* Hz, pyrimidine-CH), 6.40 (d, 1H, *J*=*9* Hz, pyrazole-CH), 6.70 (d, 1H, *J*=*8* Hz, pyrimidine-CH), 7.00 (s, 2H, Ar–H), 7.90 (d, 1H, *J*=*9* Hz, pyrazole-CH), 9.78 (s, 1H, NH), 12.58 (s, 1H, NH), 13.27 (s, 1H, NH) (Figure S15); ^{13}C-NMR (DMSO-d_6) δ ppm: 21.5 (2 C), 27.6 (2 C), 51.4 (2 C), 62.1, 101.5, 104.7, 122.2 (2 C), 125.9 (2 C), 131.8, 132.6, 133.9, 140.7, 149.2, 175.1 (Figure S16). MS (m/z, %): 351 (M^+, 57). Anal. Calced for $C_{19}H_{21}N_5S$ (351.47): C, 64.93; H, 6.02; N, 19.93%. Found: C, 64.88; H, 5.98; N, 19.86%.

6-(Pyridin-4-yl)−4-(2,3,6,7-tetrahydro-1*H*,5*H*-pyrido[3,2,1-*ij*]quinoline-9-yl)−3,4-dihydropyrimidine-2(1*H*)-thione (3 d):

Yield, 81%; m.p. 205–207 °C; IR (KBr): ν_{max}, cm^{-1}: 3315 (2 NH), 1599 (C =C), 1324 (C =S) (Figure S17); ^{1}H-NMR (DMSO-d_6) δ ppm: 1.90 (m, 4H, 2CH_2), 2.78 (t, 4H, 2CH_2), 3.61 (t, 4H, 2CH_2), 4.65 (d, 1H, *J*=*9* Hz, pyrimidine-CH), 6.98 (s, 2H, Ar–H), 7.09 (d, 1H, *J*=*9* Hz, pyrimidine-CH), 7.51 (d, 2H, *J*=*8* Hz, pyridine-CH), 8.55 (d, 2H, *J*=*8* Hz, pyridine-CH), 9.75 (s, 1H, NH), 13.60 (s, 1H, NH); ^{13}C-NMR (DMSO-d_6) δ ppm: 22.0 (2 C), 28.0 (2 C), 51.3 (2 C), 62.1, 102.0, 120.2 (2 C), 122.8 (2 C), 127.0 (2 C), 133.1, 141.0, 143.2, 149.8 (3 C), 175.8 (Figure S18). MS (m/z, %): 362 (M^+, 56). Anal. Calced for $C_{21}H_{22}N_4S$ (362.50): C, 69.58; H, 6.12; N, 15.46%. Found: C, 69.50; H, 5.98; N, 15.39%.

Synthesis of 2-thioxo-2,3-dihydropyridopyrimidine-4-one derivatives (4a-d):

General procedure

Chalcones **2a-d** (5 mmol) and 6-amino-2-thioxo-2,3-dihydropyrimidin-4(*1H*)-one (0.72 g, 5 mmol) was mixed and heated at reflux for eight hours in glacial acetic acid (20 mL). Compounds **4a–d** was obtained by cooling the reaction mixture, filtering it off, washing it with ethanol, and then recrystallizing the result from glacial acetic acid.

7-(2,3,6,7-Tetrahydro-1*H*,5*H*-pyrido[3,2,1-*ij*]quinoline-9-yl)−5-(thiazol-2-yl)−2-thioxo-2,3-dihydropyrido[2,3-*d*]pyrimidin-4(1*H*)-one (4a):

Yield, 83%; m.p. 237–239 °C; IR (KBr): ν_{max}, cm^{-1}: 3267, 3185 (2 NH), 1679 (C =O), 1627 (C =N), 1338 (C =S) (Figure S19); ^{1}H-NMR (DMSO-d_6) δ ppm: 2.00 (m, 4H, 2CH_2), 2.79 (t, 4H, 2CH_2), 3.70 (t, 4H, 2CH_2), 7.36 (d, 1H, *J*=*9* Hz, thiazole-CH), 7.70 (d, 1H, *J*=*9* Hz, thiazole-CH), 8.05 (s, 3H, 2 Ar-H + pyridine-CH), 12.30 (s, 1H, NH), 13.34 (s, 1H, NH) (Figure S20). MS (m/z, %): 433 (M^+, 53). Anal. Calced for $C_{22}H_{19}N_5OS_2$ (433.55): C, 60.95; H, 4.42; N, 16.15%. Found: C, 60.88; H, 4.37; N, 16.01%.

5-(Benzo[d]thiazol-2-yl)−7-(2,3,6,7-tetrahydro-1*H*,5*H*-pyrido[3,2,1-*ij*]quinoline-9-yl)−2-thioxo-2,3-dihydropyrido[2,3-*d*]pyrimidin-4(1*H*)-one (4b):

Yield, 79%; m.p. 253–255 °C; IR (KBr): ν_{max}, cm^{-1}: 3283, 3183 (2 NH), 1677 (C =O), 1614 (C =N), 1329 (C =S) (Figure S21); ^{13}C-NMR (DMSO-d_6) δ ppm: 23.5 (2 C), 28.5 (2 C), 52.6 (2 C), 110.5, 112.0, 122.4 (2 C), 123.5 (2 C), 124.2, 126.0 (2 C), 127.0 (2 C), 133.1, 140.8, 147.2, 150.2 (2 C), 154.1 (2 C), 161.7, 175.2 (Figure S22). MS (m/z, %): 483 (M^+, 53). Anal. Calced for $C_{26}H_{21}N_5OS_2$ (483.61): C, 64.57; H, 4.38; N, 14.48%. Found: C, 64.49; H, 4.29; N, 14.41%.

5-(1*H*-pyrazol-3-yl)−7-(2,3,6,7-tetrahydro-1*H*,5*H*-pyrido[3,2,1-*ij*]quinoline-9-yl)−2-thioxo-2,3-dihydropyrido[2,3-*d*]pyrimidin-4(1*H*)-one (4c):

Yield, 80%; m.p. 239–241 °C; IR (KBr): ν_{max}, cm^{-1}: 3253 (2 NH), 1682 (C =O), 1629 (C =N), 1329 (C =S) (Figure S23); ^{13}C-NMR (DMSO-d_6) δ ppm: 21.4 (2 C), 26.6 (2 C), 51.3 (2 C), 103.0, 110.0, 111.7, 122.0 (2 C), 125.7, 126.3 (2 C), 130.8 (2 C), 140.1, 146.7, 149.9, 153.9, 161.0, 174.8 (Figure S24). MS (m/z, %): 416 (M^+, 57), 349 (40), 244 (60), 177 (64), 172 (100), 152 (30), 102 (28), 90 (27), 87 (43), 70 (34), 66 (50) (Figure S25). Anal. Calced for $C_{22}H_{20}N_6OS$ (416.50): C, 63.44; H, 4.84; N, 20.18%. Found: C, 63.38; H, 4.77; N, 20.05%.

5-Phenyl-7-(2,3,6,7-tetrahydro-1*H*,5*H*-pyrido[3,2,1-*ij*]quinoline-9-yl)−2-thioxo-2,3-dihydropyrido[2,3-*d*]pyrimidin-4(1*H*)-one (4 d):

Yield, 73%; m.p. 218–220 °C; IR (KBr): ν_{max}, cm^{-1}: 3265, 3180 (2 NH), 1678 (C =O), 1625 (C =N), 1335 (C =S) (Figure S26); ^{1}H-NMR (DMSO-d_6) δ ppm: 1.86 (m, 4H, 2CH_2), 2.75 (t, 4H, 2CH_2), 3.60 (t, 4H, 2CH_2), 7.97 (s,

3H, 2Ar-H +pyridine-CH), 8.30 (d, 2H, *J*=*9* Hz, C_3+ C_5 pyridine-CH), 8.67 (d, 2H, *J*=*9* Hz, C_2+ C_6 pyridine-CH), 12.53 (s, 1H, NH), 13.56 (s, 1H, NH) (Figure S27). MS (m/z, %): 426 (M^+, 57). Anal. Calced for $C_{25}H_{22}N_4OS$ (426.54): C, 70.40; H, 5.20; N, 13.14%. Found: C, 70.31; H, 5.12; N, 13.01%.

Synthesis of thiazolopyrimidine 6–9 and thiazolopyridopyrimidine derivatives 10–13:

General procedure

For eight hours, a mixture of hydrazonyl chloride derivatives **5a-d** (5 mmol) and **3a-d** or **4a-d** (5 mmol) was refluxed in absolute ethanol (30 mL). Under reduced pressure, the excess solvent was removed, and the separated solid hydrochloride salt was filtered off, diluted in water, and neutralized with an aqueous sodium carbonate solution to yield the free base. To obtain the compounds **6–13**, it was filtered, washed with water, dried, and recrystallized from ethanol.

2-((4-Chlorophenyl)diazenyl)−3-methyl-5-(2,3,6,7-tetrahydro-1*H*,5*H*-pyrido[3,2,1-*ij*] quinoline-9-yl)−7-(thiazol-2-yl)−5*H*-thiazolo[3,2-*a*]pyrimidine (6a):

Yield, 74%; m.p. 224–226 °C; IR (KBr): ν_{max}, cm^{-1}: 1628 (C =N), 1572 (N =N), 783 (C–Cl) (Figure S28); ^{1}H-NMR (DMSO-d_6) δ ppm: 2.06 (m, 4H, 2CH_2), 2.27 (s, 3H, CH_3), 2.70 (t, 4H, 2CH_2), 3.60 (t, 4H, 2CH_2), 4.54 (d, 1H, *J*=*8* Hz, pyrimidine-CH), 6.70 (d, 1H, *J*=*8* Hz, pyrimidine-CH), 6.99 (s, 2H, Ar–H), 7.21 (d, 2H, *J*=*9* Hz, Ar–H, AB system), 7.44 (d, 2H, *J*=*9* Hz, Ar–H, AB system), 7.70 (d, 1H, *J*=*8* Hz, thiazole-CH), 7.80 (d, 1H, *J*=*8* Hz, thiazole-CH) (Figure S29). MS (m/z, %): 546 (M^+ + 2, 20), 544 (M^+, 59). *UV*–vis (λ_{max}): 231, 350 nm. Anal. Calced for $C_{28}H_{25}ClN_6S_2$ (545.12): C, 61.69; H, 4.62; N, 15.42%. Found: C, 61.60; H, 4.58; N, 15.38%.

3-Methyl-5-(2,3,6,7-tetrahydro-1*H*,5*H*-pyrido[3,2,1-*ij*]quinoline-9-yl)−7-(thiazol-2-yl)−2-(*p*-tolyldiazenyl)−5*H*-thiazolo[3,2-*a*]pyrimidine (6b):

Yield, 78%; m.p. 216–218 °C; IR (KBr): ν_{max}, cm^{-1}: 1610 (C =N), 1550 (N =N); ^{1}H-NMR (DMSO-d_6) δ ppm: 1.83 (m, 4H, 2CH_2), 2.20 (s, 3H, CH_3), 2.33 (s, 3H, CH_3), 2.80 (t, 4H, 2CH_2), 3.70 (t, 4H, 2CH_2), 4.49 (d, 1H, *J*=*8* Hz, pyrimidine-CH), 6.90 (d, 1H, *J*=*8* Hz, pyrimidine-CH), 7.20 (s, 2H, Ar–H), 7.41 (d, 2H, *J*=*9* Hz, Ar–H, AB system), 7.65 (d, 1H, *J*=*9* Hz, thiazole-CH), 7.73 (d, 1H, *J*=*8* Hz, thiazole-CH), 7.89 (d, 2H, *J*=*9* Hz, Ar–H, AB system) (Figure S30); ^{13}C-NMR (DMSO-d_6) δ ppm: 10.6, 21.8, 22.4 (2 C), 27.3 (2 C), 51.7 (2 C), 57.1, 93.1, 120.0, 122.0 (2 C), 127.5 (2 C), 128.5 (4 C), 133.4 (2 C), 138.3, 141.0 (2 C), 144.0 (2 C), 153.8, 159.4, 164.5 (Figure S31). MS (m/z, %): 524 (M^+, 61), 509 (31), 440 (42), 433 (61), 405 (36), 390 (33), 268 (38), 233 (31), 218 (26), 172 (100), 160 (41), 149 (28), 134 (29), 119 (42), 110 (27), 91 (22), 84 (90), 78 (33) (Figure S32). *UV*–vis (λ_{max}): 233, 355 nm. Anal. Calced for $C_{29}H_{28}N_6S_2$ (524.71): C, 66.38; H, 5.38; N, 16.02%. Found: C, 66.29; H, 5.28; N, 15.93%.

2-((4-Methoxyphenyl)diazenyl)−3-methyl-5-(2,3,6,7-tetrahydro-1*H*,5*H*-pyrido[3,2,1-*ij*]quinoline-9-yl)−7-(thiazol-2-yl)−5*H*-thiazolo[3,2-*a*]pyrimidine (6c):

Yield, 70%; m.p. 253–255 °C; IR (KBr): ν_{max}, cm^{-1}: 1621 (C =N), 1561 (N =N); ^{13}C-NMR (DMSO-d_6) δ ppm: 10.8, 22.6 (2 C), 27.5 (2 C), 52.1 (3 C), 56.0, 92.6, 113.9 (2 C), 120.4, 122.3 (2 C), 128.0 (2 C), 129.2 (2 C), 133.8 (2 C), 141.8 (2 C), 144.5 (2 C), 154.0, 159.8, 161.3, 165.5 **(Figure S33)**. MS (m/z, %): 540 (M^+, 66). *UV*–vis (λ_{max}): 230, 356 nm. Anal. Calced for $C_{29}H_{28}N_6OS_2$ (540.70): C, 64.42; H, 5.22; N, 15.54%. Found: C, 64.38; H, 5.18; N, 15.47%.

Ethyl 4-((3-methyl-5-(2,3,6,7-tetrahydro-1*H*,5*H*-pyrido[3,2,1-*ij*]quinoline-9-yl)−7-(thiazol-2-yl)−5*H*-thiazolo[3,2-*a*]pyrimidin-2-yl)diazenyl)benzoate (6 d):

Yield, 76%; m.p. 241–243 °C; IR (KBr): ν_{max}, cm^{-1}: 1715 (C =O), 1629 (C =N), 1575 (N =N) (Figure S34); ^{1}H-NMR (DMSO-d_6) δ ppm: 1.20 (t, 3H, CH_3), 1.93 (m, 4H, 2CH_2), 2.15 (s, 3H, CH_3), 2.89 (t, 4H, 2CH_2), 3.67 (t, 4H, 2CH_2), 4.21 (q, 2H, CH_2), 4.63 (d, 1H, *J*=*8* Hz, pyrimidine-CH), 6.60 (d, 1H, *J*=*8* Hz, pyrimidine-CH), 6.88 (s, 2H, Ar–H), 7.50 (d, 2H, *J*=*9* Hz, Ar–H, AB system), 7.70 (d, 1H, *J*=*8* Hz, thiazole-CH), 7.95 (d, 1H, *J*=*8* Hz, thiazole-CH), 8.05 (d, 2H, *J*=*9* Hz, Ar–H, AB system) (Figure S35). MS (m/z, %): 582 (M^+, 65). *UV*–vis (λ_{max}): 232, 357 nm. Anal. Calced for $C_{31}H_{30}N_6O_2S_2$ (582.74): C, 63.89; H, 5.19; N, 14.42%. Found: C, 63.78; H, 5.10; N, 14.37%.

7-(Benzo[d]thiazol-2-yl)−2-((4-chlorophenyl) diazenyl)−3-methyl-5-(2,3,6,7-tetrahydro-1*H*,5*H*-pyrido[3,2,1-*ij*]quinoline-9-yl)−5*H*-thiazolo[3,2-*a*] pyrimidine (7a):

Yield, 77%; m.p. 241–243 °C; IR (KBr): ν_{max}, cm^{-1}: 1630 (C =N), 1572 (N =N), 775 (C–Cl); ^{13}C-NMR (DMSO-d_6) δ ppm: 10.1, 21.0 (2 C), 26.5 (2 C), 50.2 (2 C), 56.0, 91.8, 120.0, 121.0 (3 C), 123.1 (3 C), 127.4 (2 C), 130.6 (2 C), 131.9 (2 C), 132.6 (2 C), 136.1, 141.5, 144.0, 147.1, 151.1 (2 C), 156.6, 161.8 (Figure S36). MS (m/z, %): 596 (M^+ + 2, 21), 594 (M^+, 62). *UV*–vis (λ_{max}): 231, 351 nm. Anal. Calced for $C_{32}H_{27}ClN_6S_2$ (595.18): C, 64.58; H, 4.57; N, 14.12%. Found: C, 64.50; H, 4.49; N, 14.00%.

7-(Benzo[d]thiazol-2-yl)−3-methyl-5-(2,3,6,7-tetrahydro-1*H*,5*H*-pyrido[3,2,1-*ij*]quinoline-9-yl)−2-(*p*-tolyldiazenyl)−5*H*-thiazolo[3,2-*a*]pyrimidine (7b):

Yield, 70%; m.p. 251–253 °C; IR (KBr): ν_{max}, cm^{-1}: 1630 (C =N), 1582 (N =N) (Figure S37); ^{1}H-NMR (DMSO-d_6) δ ppm: 1.95 (m, 4H, 2CH_2), 2.28 (s, 3H, CH_3), 2.39 (s, 3H, CH_3), 2.80 (t, 4H, 2CH_2), 3.60 (t, 4H, 2CH_2), 4.89

(d, 1H, *J* = *9* Hz, pyrimidine-CH), 6.65 (d, 1H, *J* = *9* Hz, pyrimidine-CH), 6.98 (s, 2H, Ar–H), 7.31 (d, 2H, *J* = *7* Hz, Ar–H, AB system), 7.50–7.65 (m, 2H, benzothiazole-CH), 7.78 (d, 2H, *J* = *7* Hz, Ar–H, AB system), 8.12 (d, 1H, *J* = *9* Hz, benzothiazole-CH), 8.36 (d, 1H, *J* = *9* Hz, benzothiazole-CH) (Figure S38). MS (m/z, %): 574 (M^+, 49). *UV*–vis (λ_{max}): 233, 351 nm. Anal. Calced for $C_{33}H_{30}N_6S_2$ (574.77): C, 68.96; H, 5.26; N, 14.62%. Found: C, 68.88; H, 5.19; N, 14.55%.

7-(Benzo[d]thiazol-2-yl)−2-((4-methoxyphenyl) diazenyl)−3-methyl-5-(2,3,6,7-tetrahydro-1*H*,5*H*-pyrido[3,2,1-*ij*]quinoline-9-yl)−5*H*-thiazolo[3,2-*a*] pyrimidine (7c):

Yield, 74%; m.p. 233–235 °C; IR (KBr): ν_{max}, cm^{-1}: 1629 (C =N), 1584 (N =N) (Figure S39); ^{1}H-NMR (DMSO-d_6) δ ppm: 1.85 (m, 4H, 2 CH_2), 2.16 (s, 3H, CH_3), 2.90 (t, 4H, 2 CH_2), 3.66 (t, 4H, 2 CH_2), 3.85 (s, 3H, O-CH_3), 4.80 (d, 1H, *J* = *8* Hz, pyrimidine-CH), 6.60 (d, 1H, *J* = *8* Hz, pyrimidine-CH), 6.90 (s, 2H, Ar–H), 7.29 (d, 2H, *J* = *8* Hz, Ar–H, AB system), 7.48–7.60 (m, 2H, benzothiazole-CH), 7.70 (d, 2H, *J* = *8* Hz, Ar–H, AB system), 8.09 (d, 1H, *J* = *9* Hz, benzothiazole-CH), 8.30 (d, 1H, *J* = *9* Hz, benzothiazole-CH) (Figure S40). MS (m/z, %): 590 (M^+, 62), 559 (50), 483 (41), 455 (31), 321 (60), 283 (45), 172 (100), 149 (53), 134 (48), 102 (34), 91 (56), 76 (48), 70 (62) (Figure S41). *UV*–vis (λ_{max}): 233, 355 nm. Anal. Calced for $C_{33}H_{30}N_6OS_2$ (590.76): C, 67.09; H, 5.12; N, 14.23%. Found: C, 67.00; H, 5.02; N, 14.12%.

Ethyl 4-((7-(benzo[d]thiazol-2-yl)−3-methyl-5-(2,3,6,7-tetrahydro-1*H*,5*H*-pyrido[3,2,1-*ij*]quinoline-9-yl)−5*H*-thiazolo[3,2-*a*]pyrimidin-2-yl)diazenyl) benzoate (7 d):

Yield, 71%; m.p. 215–217 °C; IR (KBr): ν_{max}, cm^{-1}: 1720 (C =O), 1622 (C =N), 1578 (N =N); ^{13}C-NMR (DMSO-d_6) δ ppm: 10.6, 15.8, 21.5 (2 C), 27.0 (2 C), 50.9 (3 C), 61.0, 92.0, 118.5, 119.8 (3 C), 121.8 (3 C), 126.0 (2 C), 129.2 (2 C), 130.1 (3 C), 132.4, 136.0, 140.0, 142.3, 152.0, 153.9 (2 C), 157.6, 160.3, 165.5 (Figure S42). MS (m/z, %): 632 (M^+, 69). *UV*–vis (λ_{max}): 231, 355 nm. Anal. Calced for $C_{35}H_{32}N_6O_2S_2$ (632.80): C, 66.43; H, 5.10; N, 13.28%. Found: C, 66.35; H, 4.99; N, 13.17%.

2-((4-Chlorophenyl)diazenyl)−3-methyl-7-(1*H*-pyrazol-3-yl)−5-(2,3,6,7-tetrahydro-1*H*,5*H*-pyrido[3,2,1-*ij*]quinolin-9-yl)−5*H*-thiazolo[3,2-*a*] pyrimidine (8a):

Yield, 70%; m.p. 198–200 °C; IR (KBr): ν_{max}, cm^{-1}: 3285 (NH), 1628 (C =N), 1567 (N =N), 775 (C–Cl) (Figure S43); ^{1}H-NMR (DMSO-d_6) δ ppm: 2.10 (m, 4H, 2 CH_2), 2.30 (s, 3H, CH_3), 2.80 (t, 4H, 2 CH_2), 3.53 (t, 4H, 2 CH_2), 4.49 (d, 1H, *J* = *9* Hz, pyrimidine-CH), 6.53 (d, 1H, *J* = *9* Hz, pyrimidine-CH), 6.82 (d. 1H, *J* = *8* Hz, pyrazole-CH), 7.10 (s, 2H, Ar–H), 7.35 (d, 2H, *J* = *7* Hz, Ar–H, AB system), 7.61 (d, 2H, *J* = *7* Hz, Ar–H, AB system), 7.89 (d, 1H, *J* = *9* Hz, pyrazole-CH), 12.51 (s, 1H, NH) (Figure S44). MS (m/z, %): 529 (M^+ + 2, 17), 527 (M^+, 56). *UV*–vis (λ_{max}): 233, 357 nm. Anal. Calced for $C_{28}H_{26}ClN_7S$ (528.08): C, 63.69; H, 4.96; N, 18.57%. Found: C, 63.60; H, 4.88; N, 18.50%.

3-Methyl-7-(1*H*-pyrazol-3-yl)−5-(2,3,6,7-tetrahydro-1*H*,5*H*-pyrido[3,2,1-*ij*]quinoline-9-yl)−2-(*p*-tolyldiazenyl)−5*H*-thiazolo[3,2-*a*] pyrimidine (8b):

Yield, 74%; m.p. 237–239 °C; IR (KBr): ν_{max}, cm^{-1}: 3251 (NH), 1616 (C =N), 1576 (N =N); ^{13}C-NMR (DMSO-d_6) δ ppm: 11.8, 22.5, 23.7 (2 C), 28.1 (2 C), 51.8 (2 C), 57.4, 93.7, 104.6, 120.5, 122.8 (2 C), 128.2 (2 C), 129.4 (4 C), 131.4, 134.0 (2 C), 139.2, 141.8 (2 C), 144.9, 154.1, 159.4 (Figure S45). MS (m/z, %): 507 (M^+, 57), 492 (73), 416 (40), 388 (60), 321 (48), 216 (31), 172 (100), 149 (50), 91 (73), 76 (44), 67 (33) (Figure S46). *UV*–vis (λ_{max}): 234, 358 nm. Anal. Calced for $C_{29}H_{29}N_7S$ (507.66): C, 68.61; H, 5.76; N, 19.31%. Found: C, 68.55; H, 5.66; N, 19.22%.

2-((4-Methoxyphenyl)diazenyl)−3-methyl-7-(1*H*-pyrazol-3-yl)−5-(2,3,6,7-tetrahydro-1*H*,5*H*-pyrido[3,2,1-*ij*]quinoline-9-yl)−5*H*-thiazolo[3,2-*a*] pyrimidine (8c):

Yield, 76%; m.p. 273–275 °C; IR (KBr): ν_{max}, cm^{-1}: 3257 (NH), 1623 (C =N), 1574 (N =N); ^{13}C-NMR (DMSO-d_6) δ ppm: 11.7, 23.1 (2 C), 28.0 (2 C), 53.1 (3 C), 57.0, 93.8, 104.5, 114.8 (2 C), 121.7, 123.6 (2 C), 129.0 (2 C), 130.0 (2 C), 132.1, 134.7 (2 C), 142.4 (2 C), 145.6, 155.0, 159.5, 160.8 **(Figure S47)**. MS (m/z, %): 523 (M^+, 67). *UV*–vis (λ_{max}): 231, 352 nm. Anal. Calced for $C_{29}H_{29}N_7OS$ (523.66): C, 66.52; H, 5.58; N, 18.72%. Found: C, 66.44; H, 5.50; N, 18.63%.

Ethyl 4-((3-methyl-7-(1*H*-pyrazol-3-yl)−5-(2,3,6,7-tetrahydro-1*H*,5*H*-pyrido[3,2,1-*ij*]quinoline −9-yl)−5*H*-thiazolo[3,2-*a*]pyrimidin-2-yl)diazenyl) benzoate (8 d):

Yield, 73%; m.p. 218–220 °C; IR (KBr): ν_{max}, cm^{-1}: 3302 (NH), 1728 (C =O), 1624 (C =N), 1589 (N =N) (Figure S48); ^{1}H-NMR (DMSO-d_6) δ ppm: 1.32 (t, 3H, CH_3), 2.05 (m, 4H, 2 CH_2), 2.26 (s, 3H, CH_3), 2.91 (t, 4H, 2 CH_2), 3.50 (t, 4H, 2 CH_2), 4.21 (q, 2H, CH_2), 4.55 (d, 1H, *J* = *9* Hz, pyrimidine-CH), 6.26 (d, 1H, *J* = *9* Hz, pyrimidine-CH), 6.40 (d. 1H, *J* = *8* Hz, pyrazole-CH), 6.80 (s, 2H, Ar–H), 7.31 (d, 2H, *J* = *8* Hz, Ar–H, AB system), 7.50 (d, 1H, *J* = *8* Hz, pyrazole-CH), 8.00 (d, 2H, *J* = *8* Hz, Ar–H, AB system), 12.32 (s, 1H, NH) (Figure S49). MS (m/z, %): 565 (M^+, 65). *UV*–vis (λ_{max}): 233, 358 nm. Anal. Calced for $C_{31}H_{31}N_7O_2S$ (565.70): C, 65.82; H, 5.52; N, 17.33%. Found: C, 65.77; H, 5.41; N, 17.24%.

2-((4-Chlorophenyl)diazenyl)−3-methyl-7-(pyridine-4-yl)−5-(2,3,6,7-tetrahydro-1*H*,5*H*-pyrido[3,2,1-*ij*]quinolin-9-yl)−5*H*-thiazolo[3,2-*a*]pyrimidine (9a):

Yield, 78%; m.p. 210–212 °C; IR (KBr): ν_{max}, cm^{-1}: 1619 (C = N), 1577 (N = N), 771 (C–Cl); ^{13}C-NMR (DMSO-d_6) δ ppm: 12.5, 23.4 (2 C), 29.0 (2 C), 52.5 (2 C), 58.0, 93.9, 119.5 (3 C), 121.7 (2 C), 125.9 (2 C), 129.0 (2 C), 130.0 (2 C), 131.2, 134.7, 140.0 (2 C), 142.2, 145.7, 149.5 (2 C), 155.0, 160.0 (Figure S50). MS (m/z, %): 540 (M^+ + 2, 16), 538 (M^+, 55). *UV*–vis (λ_{max}): 233, 358 nm. Anal. Calced for $C_{30}H_{27}ClN_6S$ (539.10): C, 66.84; H, 5.05; N, 15.59%. Found: C, 66.77; H, 4.91; N, 15.51%.

3-Methyl-7-(pyridin-4-yl)−5-(2,3,6,7-tetrahydro-1*H*,5*H*-pyrido[3,2,1-*ij*]quinoline-9-yl)−2-(*p*-tolyldiazenyl)−5*H*-thiazolo[3,2-*a*]pyrimidine (9b):

Yield, 71%; m.p. 230–232 °C; IR (KBr): ν_{max}, cm^{-1}: 1629 (C = N), 1580 (N = N) (Figure S51); ^{1}H-NMR (DMSO-d_6) δ ppm: 2.01 (m, 4H, 2CH_2), 2.30 (s, 3H, CH_3), 2.41 (s, 3H, CH_3), 2.77 (t, 4H, 2CH_2), 3.54 (t, 4H, 2CH_2), 4.45 (d, 1H, *J* = *9* Hz, pyrimidine-CH), 6.90 (s, 2H, Ar–H), 7.10 (d, 1H, *J* = *9* Hz, pyrimidine-CH), 7.29 (d, 2H, *J* = *7* Hz, Ar–H, AB system), 7.70 (d, 2H, *J* = *7* Hz, Ar–H, AB system), 7.97 (d, 2H, *J* = *9* Hz, C_3 + C_5 pyridine-CH), 8.58 (d, 2H, *J* = *9* Hz, C_2 + C_6 pyridine-CH) (Figure S52). MS (m/z, %): 518 (M^+, 52). *UV*–vis (λ_{max}): 232, 351 nm. Anal. Calced for $C_{31}H_{30}N_6S$ (518.68): C, 71.79; H, 5.83; N, 16.20%. Found: C, 71.70; H, 5.75; N, 16.12%.

2-((4-Methoxyphenyl)diazenyl)−3-methyl-7-(pyridin-4-yl)−5-(2,3,6,7-tetrahydro-1*H*,5*H*-pyrido[3,2,1-*ij*]quinoline-9-yl)−5*H*-thiazolo[3,2-*a*]pyrimidine (9c):

Yield, 74%; m.p. 267–269 °C; IR (KBr): ν_{max}, cm^{-1}: 1629 (C = N), 1584 (N = N) (Figure S53); ^{1}H-NMR (DMSO-d_6) δ ppm: 1.96 (m, 4H, 2CH_2), 2.25 (s, 3H, CH_3), 2.80 (t, 4H, 2CH_2), 3.50 (t, 4H, 2CH_2), 3.84 (s, 3H, O-CH_3), 4.50 (d, 1H, *J* = *9* Hz, pyrimidine-CH), 6.46 (d, 1H, *J* = *9* Hz, pyrimidine-CH), 6.98 (s, 2H, Ar–H), 7.15 (d, 2H, *J* = *7* Hz, Ar–H, AB system), 7.33 (d, 2H, *J* = *7* Hz, Ar–H, AB system), 7.98 (d, 2H, *J* = *8* Hz, C_3 + C_5 pyridine-CH), 8.51 (d, 2H, *J* = *8* Hz, C_2 + C_6 pyridine-CH) (Figure S54); ^{13}C-NMR (DMSO-d_6) δ ppm: 11.8, 24.0 (2 C), 29.8 (2 C), 51.8 (3 C), 57.4, 92.7, 114.5 (2 C), 122.2 (2 C), 126.1 (4 C), 127.9, 129.0 (2 C), 130.0 (2 C), 133.7, 137.7, 140.7 (2 C), 144.4, 154.0, 158.0, 161.3 (Figure S55). MS (m/z, %): 534 (M^+, 62), 503 (52), 427 (45), 399 (34), 321 (39), 227 (59), 172 (100), 149 (64), 135 (50), 107 (44), 78 (27), 76 (24), 51 (45) (Figure S56). *UV*–vis (λ_{max}): 233, 356 nm. Anal. Calced for $C_{31}H_{30}N_6OS$ (534.68): C, 69.64; H, 5.66; N, 15.72%. Found: C, 69.59; H, 5.59; N, 15.66%.

Ethyl 4-((3-methyl-7-(pyridin-4-yl)−5-(2,3,6,7-tetrahydro-1*H*,5*H*-pyrido[3,2,1-*ij*]quinoline-9-yl)−5*H*-thiazolo[3,2-*a*]pyrimidin-2-yl)diazenyl) benzoate (9 d):

Yield, 78%; m.p. 254–256 °C; IR (KBr): ν_{max}, cm^{-1}: 1730 (C = O), 1621 (C = N), 1551 (N = N); ^{13}C-NMR (DMSO-d_6) δ ppm: 11.2, 15.9, 23.6 (2 C), 29.1 (2 C), 51.3 (3 C), 59.9, 94.7, 120.1 (3 C), 122.4 (2 C), 126.6 (2 C), 129.9 (2 C), 130.9 (3 C), 132.0, 140.8 (2 C), 143.2, 148.0 (2 C), 153.9 (2 C), 155.9, 166.0 (Figure S57). MS (m/z, %): 576 (M^+, 55). *UV*–vis (λ_{max}): 232, 357 nm. Anal. Calced for $C_{33}H_{32}N_6O_2S$ (576.72): C, 68.73; H, 5.59; N, 14.57%. Found: C, 68.65; H, 5.49; N, 14.45%.

2-((4-Chlorophenyl)diazenyl)−3-methyl-8-(2,3,6,7-tetrahydro-1*H*,5*H*-pyrido[3,2,1-*ij*]quinoline-9-yl)−6-(thiazol-2-yl)−5*H*-pyrido[2,3-*d*]thiazolo[3,2-*a*]pyrimidin-5-one (10a):

Yield, 78%; m.p. 227–229 °C; IR (KBr): ν_{max}, cm^{-1}: 1678 (C = O), 1619 (C = N), 1573 (N = N), 798 (C–Cl) (Figure S58); ^{1}H-NMR (DMSO-d_6) δ ppm: 2.01 (m, 4H, 2CH_2), 2.31 (s, 3H, CH_3), 2.90 (t, 4H, 2CH_2), 3.54 (t, 4H, 2CH_2), 7.20 (d, 2H, *J* = *8* Hz, Ar–H, AB system), 7.38 (d, 2H, *J* = *8* Hz, Ar–H, AB system), 7.60 (d, 1H, *J* = *9* Hz, thiazole-CH), 7.80 (d, 1H, *J* = *9* Hz, thiazole-CH), 8.00 (s, 2H, Ar–H), 8.73 (s, 1H, pyridine-CH) (Figure S59). MS (m/z, %): 611 (M^+ + 2, 22), 609 (M^+, 65). *UV*–vis (λ_{max}): 230, 352 nm. Anal. Calced for $C_{31}H_{24}ClN_7OS_2$ (610.15): C, 61.02; H, 3.96; N, 16.07%. Found: C, 60.87; H, 3.90; N, 15.91%.

3-Methyl-8-(2,3,6,7-tetrahydro-1*H*,5*H*-pyrido[3,2,1-*ij*]quinoline-9-yl)−6-(thiazol-2-yl)−2-(*p*-tolyldiazenyl)−5*H*-pyrido[2,3-*d*]thiazolo[3,2-*a*]pyrimidin-5-one (10b):

Yield, 80%; m.p. 263–265 °C; IR (KBr): ν_{max}, cm^{-1}: 1670 (C = O), 1616 (C = N), 1572 (N = N); ^{13}C-NMR (DMSO-d_6) δ ppm: 12.4, 23.3, 24.1 (2 C), 29.0 (2 C), 51.9 (2 C), 93.8, 115.2, 118.3, 120.8, 122.8 (3 C), 125.0, 128.0 (2 C), 129.4 (4 C), 139.2, 141.8 (2 C), 144.9, 148.0, 154.1 (2 C), 155.2, 158.4, 165.5 (Figure S60). MS (m/z, %): 589 (M^+, 64). *UV*–vis (λ_{max}): 231, 352 nm. Anal. Calced for $C_{32}H_{27}N_7OS_2$ (589.74): C, 65.17; H, 4.61; N, 16.63%. Found: C, 65.00; H, 4.57; N, 16.56%.

2-((4-Methoxyphenyl)diazenyl)−3-methyl-8-(2,3,6,7-tetrahydro-1*H*,5*H*-pyrido[3,2,1-*ij*]quinoline-9-yl)−6-(thiazol-2-yl)−5*H*-pyrido[2,3-*d*]thiazolo[3,2-*a*]pyrimidin-5-one (10c):

Yield, 82%; m.p. 247–249 °C; IR (KBr): ν_{max}, cm^{-1}: 1679 (C = O), 1625 (C = N), 1576 (N = N); ^{13}C-NMR (DMSO-d_6) δ ppm: 12.9, 23.7 (2 C), 29.3 (2 C), 52.5 (2 C), 54.7, 94.1, 114.1 (2 C), 115.8, 117.8, 120.9, 122.9 (3 C), 125.2, 128.3 (2 C), 129.7 (2 C), 141.0 (3 C), 147.5, 153.8 (2 C), 154.4, 157.9, 161.3, 166.5 **(Figure S61)**. MS (m/z, %): 605 (M^+, 60). *UV*–vis (λ_{max}): 230, 352 nm. Anal. Calced for $C_{32}H_{27}N_7O_2S_2$ (605.74): C, 63.45; H, 4.49; N, 16.19%. Found: C, 63.39; H, 4.38; N, 16.05%.

Ethyl 4-((3-methyl-5-oxo-8-(2,3,6,7-tetrahydro-1*H*,5*H*-pyrido[3,2,1-*ij*]

quinolin-9-yl)−6-(thiazol-2-yl)−5*H*-pyrido[2,3-*d*]thiazolo[3,2-*a*]pyrimidin-2-yl)diazenyl)benzoate (10 d):

Yield, 77%; m.p. 231–233 °C; IR (KBr): ν_{max}, cm^{-1}: 1730 (C = O), 1675 (C = O), 1621 (C = N), 1574 (N = N); ^{1}H-NMR (DMSO-d_6) δ ppm: 1.40 (t, 3H, CH_3), 1.96 (m, 4H, 2 CH_2), 2.27 (s, 3H, CH_3), 2.98 (t, 4H, 2 CH_2), 3.65 (t, 4H, 2 CH_2), 4.49 (q, 2H, CH_2), 7.25 (d, 2H, *J* = *7* Hz, Ar–H, AB system), 7.40 (d, 1H, *J* = *9* Hz, thiazole-CH), 7.65 (d, 1H, *J* = *9* Hz, thiazole-CH), 7.85 (s, 2H, Ar–H), 8.07 (d, 2H, *J* = *7* Hz, Ar–H, AB system), 8.85 (s, 1H, pyridine-CH) (Figure S62). MS (m/z, %): 647 (M^+, 55), 632 (50), 618 (40), 574 (51), 563 (56), 559 (36), 490 (62), 483 (56), 455 (45), 386 (39), 371 (46), 198 (76), 172 (100), 124 (64), 104 (33), 96 (50), 84 (34), 76 (46) (Figure S63). *UV*–vis (λ_{max}): 233, 356 nm. Anal. Calced for $C_{34}H_{29}N_7O_3S_2$ (647.77): C, 63.04; H, 4.51; N, 15.14%. Found: C, 62.88; H, 4.47; N, 15.08%.

6-(Benzo[d]thiazol-2-yl)−2-((4-chlorophenyl)diazenyl)−3-methyl-8-(2,3,6,7-tetrahydro-1*H*,5*H*-pyrido[3,2,1-*ij*]quinoline-9-yl)−5*H*-pyrido[2,3-*d*]thiazolo[3,2-*a*]pyrimidin-5-one (11a):

Yield, 76%; m.p. 247–249 °C; IR (KBr): ν_{max}, cm^{-1}: 1679 (C = O), 1622 (C = N), 1578 (N = N), 760 (C–Cl); ^{13}C-NMR (DMSO-d_6) δ ppm: 11.8, 23.2 (2 C), 28.0 (2 C), 52.0 (2 C), 95.9, 118.8, 121.1 (3 C), 123.2 (2 C), 125.6 (3 C), 128.7 (2 C), 129.8 (4 C), 134.9 (2 C), 140.6 (2 C), 143.9, 147.2, 153.3, 154.0 (2 C), 157.4 (2 C), 164.0 (Figure S64). MS (m/z, %): 661 (M^+ + 2, 22), 659 (M^+, 65), 548 (39), 520 (78), 505 (60), 371 (45), 199 (59), 172 (100), 171 (30), 139 (68), 134 (49), 124 (75), 96 (72), 75 (40), 72 (24) (Figure S65). *UV*–vis (λ_{max}): 232, 355 nm. Anal. Calced for $C_{35}H_{26}ClN_7OS_2$ (660.21): C, 63.67; H, 3.97; N, 14.85%. Found: C, 63.60; H, 3.91; N, 14.74%.

6-(Benzo[d]thiazol-2-yl)−3-methyl-8-(2,3,6,7-tetrahydro-1*H*,5*H*-pyrido[3,2,1-*ij*]quinoline-9-yl)−2-(*p*-tolyldiazenyl)−5*H*-pyrido[2,3-*d*]thiazolo[3,2-*a*]pyrimidin-5-one (11b):

Yield, 73%; m.p. 277–279 °C; IR (KBr): ν_{max}, cm^{-1}: 1671 (C = O), 1620 (C = N), 1576 (N = N); ^{1}H-NMR (DMSO-d_6) δ ppm: 1.81 (m, 4H, 2 CH_2), 2.11 (s, 3H, CH_3), 2.21 (s, 3H, CH_3), 2.89 (t, 4H, 2 CH_2), 3.69 (t, 4H, 2 CH_2), 7.19 (d, 2H, *J* = *7* Hz, Ar–H, AB system), 7.39–7.50 (m, 2H, benzothiazole-CH), 7.60 (d, 2H, *J* = *7* Hz, Ar–H, AB system), 7.97 (s, 2H, Ar–H), 8.20 (d, 1H, *J* = *9* Hz, benzothiazole-CH), 8.53 (d, 1H, *J* = *9* Hz, benzothiazole-CH), 8.88 (s, 1H, pyridine-CH) (Figure S66). MS (m/z, %): 639 (M^+, 57). *UV*–vis (λ_{max}): 232, 354 nm. Anal. Calced for $C_{36}H_{29}N_7OS_2$ (639.80): C, 67.58; H, 4.57; N, 15.33%. Found: C, 67.46; H, 4.48; N, 15.27%.

6-(Benzo[d]thiazol-2-yl)−2-((4-methoxyphenyl)diazenyl)−3-methyl-8-(2,3,6,7-tetrahydro-1*H*,5*H*-pyrido[3,2,1-*ij*]quinolin-9-yl)−5*H*-pyrido[2,3-*d*]thiazolo[3,2-*a*]pyrimidin-5-one (11c):

Yield, 78%; m.p. 233–235 °C; IR (KBr): ν_{max}, cm^{-1}: 1671 (C = O), 1637 (C = N), 1578 (N = N); ^{1}H-NMR (DMSO-d_6) δ ppm: 1.78 (m, 4H, 2 CH_2), 2.17 (s, 3H, CH_3), 2.79 (t, 4H, 2 CH_2), 3.60 (t, 4H, 2 CH_2), 3.76 (s, 3H, O-CH_3), 7.10 (d, 2H, *J* = *8* Hz, Ar–H, AB system), 7.45 (d, 2H, *J* = *8* Hz, Ar–H, AB system), 7.62–7.75 (m, 2H, benzothiazole-CH), 8.09 (s, 2H, Ar–H), 8.31 (d, 1H, *J* = *9* Hz, benzothiazole-CH), 8.66 (d, 1H, *J* = *9* Hz, benzothiazole-CH), 8.99 (s, 1H, pyridine-CH) (Figure S67). MS (m/z, %): 655 (M^+, 55). *UV*–vis (λ_{max}): 230, 354 nm. Anal. Calced for $C_{36}H_{29}N_7O_2S_2$ (655.80): C, 65.93; H, 4.46; N, 14.95%. Found: C, 65.86; H, 4.39; N, 14.87%.

Ethyl 4-((6-(benzo[d]thiazol-2-yl)−3-methyl-5-oxo-8-(2,3,6,7-tetrahydro-1*H*,5*H*-pyrido[3,2,1-*ij*]quinoline-9-yl)−5*H*-pyrido[2,3-*d*]thiazolo[3,2-*a*]pyrimidin-2-yl)diazenyl)benzoate (11 d):

Yield, 71%; m.p. 254–256 °C; IR (KBr): ν_{max}, cm^{-1}: 1722 (C = O), 1677 (C = O), 1621 (C = N), 1577 (N = N) (Figure S68); ^{1}H-NMR (DMSO-d_6) δ ppm: 1.26 (t, 3H, CH_3), 1.98 (m, 4H, 2 CH_2), 2.20 (s, 3H, CH_3), 2.99 (t, 4H, 2 CH_2), 3.54 (t, 4H, 2 CH_2), 4.27 (q, 2H, CH_2), 7.31 (d, 2H, *J* = *8* Hz, Ar–H, AB system), 7.50–7.63 (m, 2H, benzothiazole-CH), 7.76 (s, 2H, Ar–H), 8.10 (d, 3H, *J* = *9* Hz, benzothiazole-CH + 2 Ar–H, AB system), 8.35 (d, 1H, *J* = *9* Hz, benzothiazole-CH), 8.70 (s, 1H, pyridine C_3-H); ^{13}C-NMR (DMSO-d_6) δ ppm: 12.1, 14.0, 23.8 (2 C), 28.5 (2 C), 51.8 (2 C), 95.6, 118.0, 120.2 (3 C), 122.3 (2 C), 124.8 (3 C), 128.0 (2 C), 129.0 (5 C), 134.1 (2 C), 140.0 (2 C), 146.5, 152.5, 153.6, 156.7 (2 C), 159.9 (2 C), 166.0 (2 C) (Figure S69). MS (m/z, %): 697 (M^+, 53). *UV*–vis (λ_{max}): 233, 355 nm. Anal. Calced for $C_{38}H_{31}N_7O_3S_2$ (697.83): C, 65.41; H, 4.48; N, 14.05%. Found: C, 65.33; H, 4.40; N, 13.92%.

2-((4-Chlorophenyl)diazenyl)−3-methyl-6-(1*H*-pyrazol-3-yl)−8-(2,3,6,7-tetrahydro-1*H*,5*H*-pyrido[3,2,1-*ij*]quinolin-9-yl)−5*H*-pyrido[2,3-*d*]thiazolo[3,2-*a*]pyrimidin-5-one (12a):

Yield, 80%; m.p. 215–217 °C; IR (KBr): ν_{max}, cm^{-1}: 3245 (NH), 1676 (C = O), 1617 (C = N), 1549 (N = N), 763 (C–Cl); ^{1}H-NMR (DMSO-d_6) δ ppm: 2.08 (m, 4H, 2 CH_2), 2.38 (s, 3H, CH_3), 2.74 (t, 4H, 2 CH_2), 3.63 (t, 4H, 2 CH_2), 6.56 (d, 1H, *J* = *9* Hz, pyrazole-CH), 7.30 (d, 2H, *J* = *9* Hz, Ar–H, AB system), 7.55 (d, 2H, *J* = *8* Hz, Ar–H, AB system), 7.74 (d, 1H, *J* = *8* Hz, pyrazole-CH), 7.97 (s, 2H, Ar–H), 8.69 (s, 1H, pyridine-CH), 12.37 (s, 1H, NH) (Figure S70); ^{13}C-NMR (DMSO-d_6) δ ppm: 12.0, 23.8 (2 C), 28.4 (2 C), 51.9 (2 C), 95.5, 102.2, 118.9, 121.4, 123.3 (2 C), 125.8, 128.9 (4 C), 129.9 (3 C), 133.5 (2 C), 142.1(2 C), 145.4, 148.9, 154.8, 155.8, 159.0, 166.0 (Figure S71). MS (m/z, %): 594 (M^+ + 2, 24), 592 (M^+, 69). *UV*–vis (λ_{max}): 233, 355 nm. Anal. Calced for $C_{31}H_{25}ClN_8OS$ (593.11):

C, 62.78; H, 4.25; N, 18.89%. Found: C, 62.70; H, 4.19; N, 18.82%.

3-Methyl-6-(1*H*-pyrazol-3-yl)−8-(2,3,6,7-tetrahydro-1*H*,5*H*-pyrido[3,2,1-*ij*]quinolin-9-yl)−2-(*p*-tolyldiazenyl)−5*H*-pyrido[2,3-*d*]thiazolo[3,2-*a*]pyrimidin-5-one (12b):

Yield, 79%; m.p. 238–240 °C; IR (KBr): ν_{max}, cm^{-1}: 3241 (NH), 1676 (C =O), 1626 (C =N), 1587 (N =N) (Figure S72); ^{13}C-NMR (DMSO-d_6) δ ppm: 11.7, 22.1, 23.2 (2 C), 27.9 (2 C), 51.8 (2 C), 93.3, 103.3, 119.3, 121.8, 123.8 (2 C), 126.0, 129.2 (2 C), 130.1 (4 C), 133.0 (2 C), 140.0, 142.4 (2 C), 145.7, 149.0, 155.2, 156.0, 159.6, 166.0 (Figure S73). MS (m/z, %): 572 (M^+, 49), 557 (50), 505 (28), 481 (47), 453 (71), 438 (67), 400 (64), 371 (74), 266 (31), 199 (25), 172 (100), 124 (46), 96 (34), 76 (37), 67 (48) (Figure S74). *UV*–vis (λ_{max}): 230, 352 nm. Anal. Calced for $C_{32}H_{28}N_8OS$ (572.69): C, 67.11; H, 4.93; N, 19.57%. Found: C, 67.00; H, 4.88; N, 19.49%.

2-((4-Methoxyphenyl)diazenyl)−3-methyl-6-(1*H*-pyrazol-3-yl)−8-(2,3,6,7-tetrahydro-1*H*,5*H*-pyrido[3,2,1-*ij*]quinolin-9-yl)−5*H*-pyrido[2,3-*d*]thiazolo[3,2-*a*]pyrimidin-5-one (12c):

Yield, 73%; m.p. 221–223 °C; IR (KBr): ν_{max}, cm^{-1}: 3244 (NH), 1679 (C =O), 1622 (C =N), 1580 (N =N); ^{13}C-NMR (DMSO-d_6) δ ppm: 11.7, 22.1 (2 C), 27.9 (2 C), 51.8 (2 C), 53.9, 95.4, 102.7, 115.8 (2 C), 118.8, 122.0, 124.0 (2 C), 126.1, 129.7 (2 C), 130.5 (2 C), 133.9 (2 C), 142.0 (3 C), 148.2, 154.5, 155.7, 158.8, 162.4, 167.8 (Figure S75). MS (m/z, %): 588 (M^+, 53). *UV*–vis (λ_{max}): 232, 353 nm. Anal. Calced for $C_{32}H_{28}N_8O_2S$ (588.69): C, 65.29; H, 4.79; N, 19.03%. Found: C, 65.20; H, 4.72; N, 18.91%.

Ethyl 4-((3-methyl-5-oxo-6-(1*H*-pyrazol-3-yl)−8-(2,3,6,7-tetrahydro-1*H*,5*H*-pyrido[3,2,1-*ij*]quinolin-9-yl)−5*H*-pyrido[2,3-*d*]thiazolo[3,2-*a*]pyrimidin-2-yl) diazenyl)benzoate (12 d):

Yield, 74%; m.p. 262–264 °C; IR (KBr): ν_{max}, cm^{-1}: 3240 (NH), 1725 (C =O), 1672 (C =O), 1624 (C =N), 1578 (N =N); ^{1}H-NMR (DMSO-d_6) δ ppm: 1.48 (t, 3H, CH_3), 1.96 (m, 4H, 2CH_2), 2.28 (s, 3H, CH_3), 2.66 (t, 4H, 2CH_2), 3.60 (t, 4H, 2CH_2), 4.37 (q, 2H, CH_2), 6.61 (d, 1H, *J*=*9* Hz, pyrazole-CH), 7.39 (d, 2H, *J*=*7* Hz, Ar–H, AB system), 7.81 (d, 1H, *J*=*9* Hz, pyrazole-CH), 8.02 (s, 2H, Ar–H), 8.10 (d, 2H, *J*=*7* Hz, Ar–H, AB system), 8.78 (s, 1H, pyridine-CH), 12.49 (s, 1H, NH) (Figure S76). MS (m/z, %): 630 (M^+, 59). *UV*–vis (λ_{max}): 232, 355 nm. Anal. Calced for $C_{34}H_{30}N_8O_3S$ (630.73): C, 64.75; H, 4.79; N, 17.77%. Found: C, 64.69; H, 4.71; N, 17.68%.

2-((4-chlorophenyl)diazenyl)−3-methyl-6-(pyridin-4-yl)−8-(2,3,6,7-tetrahydro-1*H*,5*H*-pyrido[3,2,1-*ij*]quinolin-9-yl)−5*H*-pyrido[2,3-*d*]thiazolo[3,2-*a*]pyrimidin-5-one (13a):

Yield, 78%; m.p. 266–268 °C; IR (KBr): ν_{max}, cm^{-1}: 1670 (C =O), 1618 (C =N), 1570 (N =N), 762 (C–Cl); ^{13}C-NMR (DMSO-d_6) δ ppm: 10.1, 21.9 (2 C), 26.5 (2 C), 53.0 (2 C), 95.6, 116.5, 120.0, 122.2 (2 C), 124.5 (2 C), 126.7 (3 C), 130.0 (2 C), 131.0 (2 C), 136.1, 142.0 (3 C), 145.1, 148.3 (3 C), 154.5, 155.5, 158.7, 165.7 (Figure S77). MS (m/z, %): 605 (M^+ + 2, 22), 603 (M^+, 65). *UV*–vis (λ_{max}): 232, 354 nm. Anal. Calced for $C_{33}H_{26}ClN_7OS$ (604.13): C, 65.61; H, 4.34; N, 16.23%. Found: C, 65.55; H, 4.27; N, 16.16%.

3-methyl-6-(pyridin-4-yl)−8-(2,3,6,7-tetrahydro-1*H*,5*H*-pyrido[3,2,1-*ij*]quinolin-9-yl)−2-(*p*-tolyldiazenyl)−5*H*-pyrido[2,3-*d*]thiazolo[3,2-*a*]pyrimidin-5-one (13b):

Yield, 71%; m.p. 229–231 °C; IR (KBr): ν_{max}, cm^{-1}: 1673 (C =O), 1621 (C =N), 1577 (N =N); ^{1}H-NMR (DMSO-d_6) δ ppm: 1.86 (m, 4H, 2CH_2), 2.20 (s, 3H, CH_3), 2.28 (s, 3H, CH_3), 2.86 (t, 4H, 2CH_2), 3.60 (t, 4H, 2CH_2), 7.29 (d, 2H, *J*=*9* Hz, Ar–H, AB system), 7.70 (d, 2H, *J*=*9* Hz, Ar–H, AB system), 7.92 (s, 2H, Ar–H), 8.16 (d, 2H, *J*=*9* Hz, C_3 + C_5 pyridine-CH), 8.61 (s, 1H, pyridine-CH), 8.80 (d, 2H, *J*=*9* Hz, C_2 + C_6 pyridine-CH) (Figure S78); ^{13}C-NMR (DMSO-d_6) δ ppm: 10.3, 21.6, 22.8 (2 C), 27.7 (2 C), 51.5 (2 C), 96.0, 117.5, 120.7, 121.8 (2 C), 123.9, 126.0 (2 C), 129.6 (2 C), 130.3 (4 C), 138.1 (2 C), 142.5 (2 C), 145.8, 149.1 (3 C), 155.2, 156.0, 159.7, 166.1 (Figure S79). MS (m/z, %): 583 (M^+, 59). *UV*–vis (λ_{max}): 230, 353 nm. Anal. Calced for $C_{34}H_{29}N_7OS$ (583.71): C, 69.96; H, 5.01; N, 16.80%. Found: C, 69.87; H, 4.90; N, 16.72%.

2-((4-methoxyphenyl)diazenyl)−3-methyl-6-(pyridin-4-yl)−8-(2,3,6,7-tetrahydro-1*H*,5*H*-pyrido[3,2,1-*ij*]quinolin-9-yl)−5*H*-pyrido[2,3-*d*]thiazolo[3,2-*a*]pyrimidin-5-one (13c):

Yield, 70%; m.p. 241–243 °C; IR (KBr): ν_{max}, cm^{-1}: 1672 (C =O), 1620 (C =N), 1576 (N =N); ^{1}H-NMR (DMSO-d_6) δ ppm: 1.80 (m, 4H, 2CH_2), 2.10 (s, 3H, CH_3), 2.80 (t, 4H, 2CH_2), 3.59 (t, 4H, 2CH_2), 3.81 (s, 3H, O-CH_3), 7.18 (d, 2H, *J*=*8* Hz, Ar–H, AB system), 7.31 (d, 2H, *J*=*8* Hz, Ar–H, AB system), 7.81 (s, 2H, Ar–H), 8.03 (d, 2H, *J*=*9* Hz, C_3 + C_5 pyridine-CH), 8.50 (s, 1H, pyridine-CH), 8.69 (d, 2H, *J*=*9* Hz, C_2 + C_6 pyridine-CH) (Figure S80). MS (m/z, %): 599 (M^+, 48), 584 (60), 521 (46), 492 (49), 464 (67), 449 (78), 386 (29), 371 (69), 214 (40), 199 (20), 172 (100), 135 (57), 124 (55), 92 (35), 78 (22), 76 (33) (Figure S81). *UV*–vis (λ_{max}): 231, 355 nm. Anal. Calced for $C_{34}H_{29}N_7O_2S$ (599.71): C, 68.09; H, 4.87; N, 16.35%. Found: C, 68.00; H, 4.81; N, 16.26%.

Ethyl 4-((3-methyl-5-oxo-6-(pyridin-4-yl)−8-(2,3,6,7-tetrahydro-1*H*,5*H*-pyrido[3,2,1-*ij*] quinoline-9-yl)−5*H*-pyrido[2,3-*d*]thiazolo[3,2-*a*]pyrimidin-2-yl) diazenyl)benzoate (13 d):

Yield, 74%; m.p. 232–234 °C; IR (KBr): ν_{max}, cm^{-1}: 1715 (C =O), 1658 (C =O), 1628 (C =N), 1572 (N =N) (Figure S82); ^{13}C-NMR (DMSO-d_6) δ ppm: 12.8, 14.8, 24.2 (2 C), 29.1 (2 C), 52.2 (2 C), 96.0, 117.7, 119.9, 121.9 (2 C),

124.0 (3 C), 127.6 (3 C), 128.2 (5 C), 139.7 (3 C), 146.0 (3 C), 152.0, 152.9, 156.0, 159.5, 165.6 (2 C) (Figure S83). MS (m/z, %): 641 (M^+, 55). *UV*–vis (λ_{max})(Figure S84): 231, 354 nm. Anal. Calced for $C_{36}H_{31}N_7O_3S$ (641.75): C, 67.38; H, 4.87; N, 15.28%. Found: C, 67.29; H, 4.82; N, 15.19%.

Antimicrobial activity

The cup agar diffusion method was used to evaluate the integrated mixes'antimicrobial movement [48]. Three test microorganisms that were representative of each group were used: yeast (*C. albicans* ATCC 10231), G-ve bacteria (*E. coli* ATCC 25933), and G + ve bacteria (*S. aureus* ATCC 6538-P). On nutritional agar medium plates, test microorganisms and bacteria were injected with 0.1 ml of 10^5–10^6 cells/ml. To assess the antifungal activity, 0.1 ml (106 cells/ml) of the fungal inoculum was planted into potato dextrose agar plates. In every infected plate, wells were started. Each cup contained 100 µl of each sample. After that, plates were stored for two to four hours at a low temperature (4 °C) to allow for the greatest possible dispersion. The plates were then incubated for 24 h at 37 °C for bacteria and 48 h at 30 °C for the fungus, with the temperature carefully adjusted to allow for the maximum possible development of the organisms. By determining the width of the zone of inhibition that was transmitted in millimeters (mm), the test specialist's antibacterial action was assessed. At least one or two trials were finished, and the average number of inhibition zone was noted.

Determination of MIC of the most active compounds

Mueller Hinton medium was used to cultivate *Staphylococcus aureus* ATCC 6538, *Escherichia coli* ATCC 25933, and MRSA. Fresh bacterial cell pellets were suspended in 20 mL of sterile saline. The turbidity of the bacterial suspension was measured at 500 nm and adjusted to an optical density corresponding to 0.5–1.0 at OD500 McFarland standard using aseptic techniques. A final inoculum concentration of 5×10^6 CFU/mL was prepared. To perform the resazurin-based microdilution assay, 67.5 mg of resazurin was dissolved in 10 mL of sterile distilled water, stirred thoroughly using a vortex mixer, and filtered through a 0.22 µm membrane. The resulting solution was used as the viability indicator. In a sterile 96-well microplate, 50 µL of each test compound (5 mg/mL stock solution) was added to the first column, followed by serial two-fold dilutions across the row. Then, 100 µL of the bacterial suspension (5×10^6 CFU/mL) and 100 µL of the resazurin solution were added to each well. Plates were prepared in duplicate and incubated at 37 °C for 18–24 h. The color change was visually observed. A shift in color from purple to pink or colorless indicated bacterial growth. The MIC was defined as the lowest concentration of the compound at which no visible color change occurred [49].

Molecular docking study

The benzothiazole derivatives inhibited the *E. coli* Gyr B enzyme (PDB ID 1aj6) from working well [50]. To utilized M.O.E. 2019.01 to conduct molecular docking experiments on the X-ray crystal structure of the (PDB ID: 1aj6) protein to investigate the interactions between the produced benzothiazole derivatives. Through the preparation of protein hydrogen atoms were added to the structure to correct protonation states while both of Water molecules and heteroatoms were removed to simplify the system in addition the structure was energy-minimized using the AMBER10:EHT force field to relieve steric clashes. Meanwhile, through the preparation of ligand the energy was minimized using the MMFF94x force field, and partial charges were assigned. Besides, the docking protocol was validated by re-docking the co-crystallized ligand into the binding site of the prepared protein. The root-mean-square deviation (RMSD) between the docked pose and the crystallographic pose was calculated to be 1.2 Å, confirming the reliability of the docking methodology.

Methodology of molecular modeling

Using Gaussian 09 [51] software as an advanced program that applied to optimize the structures to obtain the best distribution of atoms as well as some essential physical properties which support some experimental data. The polarization basis set of valence double-zeta (6-31G*) was the used for the modeling process under DFT/B3LYP method [52, 53]. The obtained files were visualized by Gauss-View and Gauss-Sum 2.2 [54].

Conclusion

The synthesis and evaluation of a series of thiazolopyrimidine derivatives, as described in this study, successfully demonstrate the potential of these compounds for biological and pharmacological applications. The multi-step synthetic route employed to prepare chalcones, pyrimidinethions, pyridopyrimidines, and their subsequent transformations with hydrazonyl chlorides resulted in the generation of forty novel thiazolopyrimidine derivatives. These compounds were thoroughly characterized through elemental and spectral analysis, confirming their structures. In vitro antibacterial testing revealed that compounds **7a**, **7b**, **11a**, and **11b** exhibited the highest antibacterial activity against both

Gram-positive *S. aureus* and Gram-negative *E. coli*, as well as moderate activity against *C. albicans*. Docking studies further supported the promising activity of these derivatives, suggesting specific binding interactions with the target protein (PDB: 1aj6), which could explain their selective antibacterial properties. Overall, this work highlights the potential of thiazolopyrimidine derivatives as effective antibacterial agents, with distinct binding profiles that may be exploited for further drug development. Furthermore, DFT-based molecular modeling confirmed the stability and high electronic reactivity of selected bioactive compounds, with low HOMO–LUMO energy gaps and favorable electrostatic potential profiles.

Supplementary Information

The online version contains supplementary material available at https://doi.org/10.1186/s13065-025-01506-1.

Additional file1

Acknowledgements
There is no acknowledgements, there is no funding source

Author contributions
Author Contribution—CRediT Taxonomy: Jihan Qurban1, Sara A. Alqarni2: Data curation, formal analysis, methodology, and software; Adel I. Alalawy3, Nawaa Ali H. Alshammari4: Investigation and writing—review & editing; Gadeer R. S. Ashour1, Maryam M. Alnoman5: formal analysis, investigation, writing-original draft. Hanadi A. Katuah1 and Nashwa M. El-Metwaly: Supervision and administration of research group.

Funding
No funding source is a personal funding.

Availability of data and materials
All relevant data are within the manuscript and available from the corresponding author upon request.

Declarations

Ethical approval and consent to participate
Not applicable and all authors participated directly in the current research work.

Consent for publication
Not Applicable.

Competing interests
The authors declare no competing interests.

Received: 2 January 2025 Accepted: 12 May 2025
Published online: 28 May 2025

References:

1. Gomtsyan A. Heterocycles in drugs and drug discovery. Chem Heterocycl Compd. 2012;48:7–10. https://doi.org/10.1007/s10593-012-0960-z.
2. Lord RM, Holmes J, Singer FN, Frith A, Willans CE. Precious metal n-heterocyclic carbene-carbaboranyl complexes: cytotoxic and selective compounds for the treatment of cancer. J Organometal Chem. 2019;907:121062–75. https://doi.org/10.1016/j.jorganchem.2019.121062.
3. Wang S, Bao L, Song D, Wang J, Cao X. Heterocyclic lactam derivatives containing piperonyl moiety as potential antifungal agents. Bioorg Med Chem Lett. 2019;29(20):126661–5. https://doi.org/10.1016/j.bmcl.2019.126661.
4. Fayed EA, Mohsen M, Abd El-Gilil SM, Aboul-Magd DS, Ragab A. Novel cyclohepta[b]thiophene derivative incorporating pyrimidine, pyridine, and chromene moiety as potential antimicrobial agents targeting DNA gyrase. J Mol Struct. 2022;1262:133028. https://doi.org/10.1016/j.molstruc.2022.133028.
5. Ragab A, Abusaif MS, Aboul-Magd DS, Wassel MM, Elhagali GA, Ammar YA. A new exploration toward adamantane derivatives as potential anti-MDR agents: design, synthesis, antimicrobial, and radiosterilization activity as potential topoisomerase IV and DNA gyrase inhibitors. Drug Dev Res. 2022;83(6):1305–30. https://doi.org/10.1002/ddr.21960.
6. Ragab A, Abusaif MS, Gohar NA, Aboul-Magd DS, Fayed EA, Ammar YA. Development of new spiro[1,3]dithiine-4,11′-indeno[1,2-b]quinoxaline derivatives as S. aureus sortase a inhibitors and radiosterilization with molecular modeling simulation. Bioorg Chem. 2023;131:106307. https://doi.org/10.1016/j.bioorg.2022.106307.
7. Baril A, Grenier D, Azelmat J, Syed SA, Al Obaid AM, Hosten EC. Synthesis and anti-inflammatory activity of diversified heterocyclic systems. Chem Biol Drug Des. 2019;94(4):1750–9. https://doi.org/10.1111/cbdd.13576.
8. Rawat P, Verma SM, Kumar P. Novel chroman analogs as promising heterocyclic compounds: their synthesis and antiepileptic activity. Ind J Pharma Edu Res. 2019;53:655–65. https://doi.org/10.5530/ijper.53.4s.162.
9. Shakurova ER, Parfenova LV. Synthesis of N-heterocyclic analogues of 28-O methyl betulinate and their antibacterial and antifungal properties. Molbank. 2019;2020(1):M1100. https://doi.org/10.3390/M1100.
10. Ragab A, Fouad SA, Ammar YA, Aboul-Magd DS, Abusaif MS. Antibiofilm and anti-quorum-sensing activities of novel pyrazole and pyrazolo[1,5-a] pyrimidine derivatives as carbonic anhydrase I and II inhibitors: design, synthesis, radiosterilization, and molecular docking studies. Antibiotics. 2023;12(1):128. https://doi.org/10.3390/antibiotics12010128.
11. Abdelgalil MM, Ammar YA, Ali GAE, Ali AK, Ragab A. A novel of quinoxaline derivatives tagged with pyrrolidinyl scaffold as a new class of antimicrobial agents: design, synthesis, antimicrobial activity, and molecular docking simulation. J Mol Struct. 2023;1274: 134443. https://doi.org/10.1016/j.molstruc.2022.134443.
12. Kumar S, Deep A, Narasimhan B. A review on synthesis, anticancer and antiviral potentials of pyrimidine derivatives. Curr Bioact Compd. 2019;15(3):289–303. https://doi.org/10.2174/1573407214666180124160405.
13. Madia VN, Nicolai A, Messore A, De Leo A, Ialongo D, Tudino V, Saccoliti F, De Vita D, Scipione L, Artico M, Taurone S. Design, synthesis and biological evaluation of new pyrimidine derivatives as anticancer agents. Molecules. 2021;26(3):771. https://doi.org/10.3390/molecules26030771.
14. Ahmed K, Choudhary MI, Saleem RSZ. Heterocyclic pyrimidine derivatives as promising antibacterial agents. Eur J Med Chem. 2023. https://doi.org/10.1016/j.ejmech.2023.115701.
15. Irshad N, Khan AU, Iqbal MS. Antihypertensive potential of selected pyrimidine derivatives: explanation of underlying mechanistic pathways. Biomed Pharmacother. 2021;139: 111567. https://doi.org/10.1016/j.biopha.2021.111567.
16. Maurya SS, Khan SI, Bahuguna A, Kumar D, Rawat DS. Synthesis, antimalarial activity, heme binding and docking studies of N-substituted 4-aminoquinoline-pyrimidine molecular hybrids. Eur J Med Chem. 2017;129:175–85. https://doi.org/10.1016/j.ejmech.2017.02.024.
17. Azeredo LFS, Coutinho JP, Jabor VA, Feliciano PR, Nonato MC, Kaiser CR, Menezes CMS, Hammes AS, Caffarena ER, Hoelz LV, de Souza NB. Evaluation of 7-arylaminopyrazolo [1, 5-a] pyrimidines as anti-plasmodium falciparum, antimalarial, and pf-dihydroorotate dehydrogenase inhibitors. Eur J Med Chem. 2017;126:72–83. https://doi.org/10.1016/j.ejmech.2016.09.073.
18. Maddila S, Gorle S, Seshadri N, Lavanya P, Jonnalagadda SB. Synthesis, antibacterial and antifungal activity of novel benzothiazole pyrimidine derivatives. Arab J Chem. 2016;9(5):681–7. https://doi.org/10.1016/j.arabjc.2013.04.003.
19. Patil AD, Kumar NV, Kokke WC, Bean MF, Freyer AJ, Brosse CD, Mai S, Truneh A, Carte B. Novel alkaloids from the sponge Batzella Sp.: inhibitors of HIV Gp120-Human CD4 binding. J Org Chem. 1995;60(5):1182–8. https://doi.org/10.1021/jo00110a021.

20. Pawar S, Kumar K, Gupta MK, Rawal RK. Synthetic and medicinal perspective of fused-thiazoles as anticancer agents. Anti-Cancer Agents Med Chem. 2021;21(11):1379–402. https://doi.org/10.2174/1871520620666200728133017.
21. Chhabria T, Patel M, Modi P, Brahmkshatriya PS. Thiazole: a review on chemistry, synthesis and therapeutic importance of its derivatives. Curr Top Med Chem. 2016;16(26):2841–62. https://doi.org/10.2174/1568026616666160506130731.
22. Singh S, Schober A, Michael G, Alexander AG. Convenient method for synthesis of thiazolo [3, 2-a] pyrimidine derivatives in a one-pot procedure. Tetrahedron Lett. 2011;52(29):3814–7. https://doi.org/10.1016/j.tetlet.2011.05.067.
23. Kulakov IV, Nurkenov OA, Turdybekov DM, Issabaeva GM, Mahmutova AS, Turdybekov KM. Synthesis of thiazolo [3, 2-a] pyrimidines based on 4-Aryl-substituted 3, 4-dihydro-pyrimidine (1H)-2-thiones and the crystal structure of ethyl 5-(2, 4-Dimethoxyphenyl)-7-methyl-3-Oxo-3, 5-Dihydro-2H-Thiazolo-[3, 2-a] Pyrimidine-6-Carboxylate. Chem Heterocycl Compd. 2009;45(7):856–9. https://doi.org/10.1007/s10593-009-0346-z.
24. Ozair A, Suroor AK, Nadeem S, Waquar A, Suraj PV, Sadaf JG. antihypertensive activity of newer 1, 4-Dihydro-5-pyrimidine carboxamides: synthesis and pharmacological evaluation. Eur J Med Chem. 2010;45(11):5113–9. https://doi.org/10.1016/j.ejmech.2010.08.022.
25. Mohamed SF, Flefel EM, Amr AEGE, Abd El-Shafy DN. Anti-HSV-1 activity and mechanism of action of some new synthesized substituted pyrimidine Thiopyrimidine and Thiazolopyrimidine Derivatives. Eur J Med Chem. 2010;45(4):1494–501. https://doi.org/10.1016/j.ejmech.2009.12.057.
26. Selvam TP, Karthik V, Kumar PV, Ali MA. Design, synthesis, antinociceptive, and anti-inflammatory properties of thiazolopyrimidine derivatives. Toxicol Environ Chem. 2012;94(7):1247–58. https://doi.org/10.1080/02772248.2012.703204.
27. Tantak NP, Chaudhari S. Degradation of azo dyes by sequential fenton's oxidation and aerobic biological treatment. J Hazard Mater. 2006;136(3):698–705. https://doi.org/10.1016/j.jhazmat.2005.12.049.
28. Bentley R. Different roads to discovery; prontosil (Hence Sulfa Drugs) and penicillin (Hence β-Lactams). J Ind Microbiol Biotechnol. 2009;36(6):775–86. https://doi.org/10.1007/s10295-009-0553-8.
29. Abdel-Aziem A, El-Gendy MS, Abdelhamid AO. Synthesis and antimicrobial activities of pyrido [2, 3-D] pyrimidine, pyridotriazolopyrimidine, triazolopyrimidine, and Pyrido [2, 3-D: 6, 5-D'] dipyrimidine derivatives. Eur J Chem. 2012;3(4):455–60. https://doi.org/10.5155/eurjchem.3.4.455-460.683.
30. Hayallah AM, Abdel-Hamid MK. Design and synthesis of new pyrido [2, 3-D] pyrimidine-1, 4-dione derivatives as anti-inflammatory agents. Der Pharm Chem. 2014;6(5):45–57.
31. Pedeboscq S, Gravier D, Casadebaig F, Hou G, Gissot A, Giorgi FD, Ichas F, Cambar J, Pometan JP. Synthesis and study of antiproliferative activity of novel thienopyrimidines on glioblastoma cells. Eur J Med Chem. 2010;45(6):2473–9. https://doi.org/10.1016/j.ejmech.2010.02.032.
32. Ouf NH, Amr AE. Synthesis and anti-inflammatory activity of some pyrimidines and thienopyrimidines using 1-(2-Benzo [D][1, 3] Dioxol-5-Yl) Vinyl)-4-Mercapto-6-Methylpyrimidine-5-Yl) Ethan-2-One as a Starting Material. Monatsh Chem. 2008;139:579–85. https://doi.org/10.1007/s00706-007-0793-0.
33. Cueto-Díaz EJ, Ebiloma GU, Alfayez IA, Ungogo MA, Lemgruber L, González-García MC, Giron MD, Salto R, Fueyo-González FJ, Shiba T, González-Vera JA. Synthesis, biological, and photophysical studies of molecular rotor-based fluorescent inhibitors of the trypanosome alternative oxidase. Eur J Med Chem. 2021;220: 113470. https://doi.org/10.1016/j.ejmech.2021.113470.
34. El Gendy MAM, Hassanein H, Saleh FM, Karimi-Busheri F, Fanta M, Yang X, Tawfik D, Morsy S, Fahmy M, Hemid M, Abdel Azeiz M, Fared A, Weinfeld M. Hydrazonoyl chlorides possess promising antitumor properties. Life Sci. 2022;295: 120380. https://doi.org/10.1016/j.lfs.2022.120380.
35. Świątek K, Utecht-Jarzyńska G, Palusiak M, Ma JA, Jasiński M. One-pot synthesis of 1-Aryl-3-Trifluoromethylpyrazoles using nitrile imines and mercaptoacetaldehyde as a surrogate of acetylene. Org Lett. 2023;25(24):4462–7. https://doi.org/10.1021/acs.orglett.3c01437.
36. Mosselhi MAN, Abdallah MA, Mohamed YF, Shawali AS. synthesis and tautomeric structure of 7-arylhydrazono-7H-[1, 2, 4] Triazolo [3, 4-B][1, 3, 4] thiadiazines, phosphorus, sulfur. Silicon Relat Elem. 2002;177(2):487–96. https://doi.org/10.1080/10426500210251.
37. Bayoumy NM, Fadda AA, Soliman NN. Dyeing performance on polyester fibers and DFT investigation of newly synthesized 2-Arylazo-dioxoisoindolinecyanoacetamide derivatives. J Text Inst. 2024;115(9):1621–32. https://doi.org/10.1080/00405000.2023.2258746.
38. Rollas S, Gulerman N, Erdeniz H. Synthesis and antimicrobial activity of some new hydrazones of 4-fluorobenzoic acid hydrazide and 3-acetyl-2, 5-disubstituted-1, 3, 4-oxadiazolines. Il Farmaco. 2002;57(2):171–4. https://doi.org/10.1016/S0014-827X(01)01192-2.
39. Al-Hazmi GAA, Abou-Melha KS, El-Metwaly NM, Althagafi I, Shaaban F, Zaki R. Green synthesis approach for Fe(III), Cu(II), Zn(II) and Ni(II)-Schiff base complexes, spectral, conformational, MOE-docking and biological studies. Appl Organomet Chem. 2020;34: e5403. https://doi.org/10.1002/aoc.5403.
40. Anderson JSM, Melin J, Ayers PW. Conceptual density-functional theory for general chemical reactions, including those that are neither charge-nor frontier-orbital-controlled. 2. Application to molecules where frontier molecular orbital theory fails. Comput Theor Chem. 2007;3(2):375–89. https://doi.org/10.1021/ct6001658.
41. Abumelha HM, Al-Fahemi JH, Althagafi I, Bayazeed AA, Al-Ahmed ZA, Khedr AM, El-Metwaly NM. Deliberate-characterization for Ni(II)-Schiff base complexes: promising in-vitro anticancer feature that matched MOE docking-approach. J Inorg Organomet Polym Mater. 2020;30(9):3277–93. https://doi.org/10.1007/s10904-020-01503-y.
42. Raman N, Muthuraj V, Ravichandran S, Kulandaisamy A. Synthesis, characterization and electrochemical behaviour of Cu(II), Co(II), Ni(II) and Zn(II) complexes derived from acetylacetone and p-anisidine and their antimicrobial activity. Proc Indian Acad Sci. 2003;115:161–7. https://doi.org/10.1007/BF02704255.
43. Yousef TA, El-Reash GMA, El-Gammal OA, Ahmed SF. Structural, DFT and biological studies on Cu(II) complexes of semi and thiosemicarbazide ligands derived from diketo hydrazide. Polyhedron. 2014;81:749–63. https://doi.org/10.1016/j.poly.2014.07.035.
44. Kudale VS, Wang J-J. Metal-free C-H methylation and acetylation of heteroarenes with PEG-400. Green Chem. 2020;22(11):3506–11. https://doi.org/10.1039/D0GC01183E.
45. Fries RW, Bohlken DP, Plapp BV. 3-Substituted pyrazole derivatives as inhibitors and inactivators of liver alcohol dehydrogenase. J Med Chem. 1979;22(4):356–9. https://doi.org/10.1021/jm00190a005.
46. Kumar P, Das S. Kinetics and adsorption isotherm model of 2-thiouracil adsorbed onto the surface of reduced graphene oxide-copper oxide nanocomposite material. J Mol Struct. 2022;1268: 133723. https://doi.org/10.1016/j.molstruc.2022.133723.
47. Moussa Z, Paz AP, Khalaf MA, Judeh ZMA, Alzamly A, Samadi A, Al-Fahemi JH, et al. First exclusive stereo- and regioselective preparation of 5-arylimino-1,3,4-selenadiazole derivatives: synthesis, NMR analysis, and computational studies. Chem Asian J. 2023;18(17): e202300475. https://doi.org/10.1002/asia.202300475.
48. Abo-Salem HM, Abd El Salam HA, Abdel-Aziem A, Abdel-Aziz MS, El-Sawy ER. Synthesis, molecular docking, and biofilm formation inhibitory activity of bis (Indolyl) pyridines analogues of the marine alkaloid nortopsentin. Molecules. 2021;26(14):4112. https://doi.org/10.3390/molecules26144112.
49. Sarker SD, Nahar L, Kumarasamy Y. Microtitre plate-based antibacterial assay incorporating Resazurin as an indicator of cell growth, and its application in the in vitro antibacterial screening of phytochemicals. Methods. 2007;42(4):321–4. https://doi.org/10.1016/j.ymeth.2007.01.006.
50. Jayaram U, Azam MA, Rajeshkumar R. Synthesis, molecular docking and antibacterial activity evaluation of some novel 3,7-Disubstituted-[1,3] Thiazolo[4,5-D]Pyrimidin-2(3H)-One Derivatives. FABAD J Pharm Sci. 2018;43(3):249–61.
51. M. Frisch, F. Clemente, Gaussian 09, Revision A.01, M.J. Frisch, G.W. Trucks, H.B. Schlegel, G.E. Scuseria, M.A. Robb, J.R. Cheeseman, G. Scalmani, V. Barone, B. Mennucci, G.A. Petersson, H. Nakatsuji, M. Caricato, X. Li, H.P. Hratchian, A.F. Izmaylov, J. Bloino, G. Zhe, (2009) 20–44.
52. Lee C, Yang W, Parr RG. Development of the Colle-Salvetti correlation-energy formula into a functional of the electron density. Phys Rev B. 1988;37:785–9. https://doi.org/10.1103/PhysRevB.37.785.

53. Becke AD. Density-functional thermochemistry. III. The role of exact exchange. J Chem Phys. 1993;98:5648–52. https://doi.org/10.1063/1.464913.
54. R. Dennington, T. Keith, J. Millam, GaussView, Ver. 4.1, Semichem Inc., Shawnee Mission, KS (2009).

Publisher's Note